EVALUATION AND VALIDATION OF COMPUTED TOMOGRAPHY DOSE ACCURACY

($CTDI_w$ AND $CTDI_{vol}$)

This thesis is submitted to the:

DEPARTMENT OF MEDICAL PHYSICS
SCHOOL OF NUCLEAR AND ALLIED SCIENCES
UNIVERSITY OF GHANA, LEGON

BY

ABROKWA ABOAGYE SINTIM

(10285253)

In partial fulfilment of the requirement for the award of

MASTER OF PHILOSOPHY

IN

MEDICAL PHYSICS

JULY, 2016

DECLARATION

This thesis is the result of research work undertaken by Abrokwa Aboagye Sintim in the Department of Medical Physics, University of Ghana, under the supervision of Prof. Augustine Kwame Kyere, Dr. Francis Hasford and Mr. Edem Kwabla Sosu.

It is my conviction that, no part of this work has been presented in part or whole to any other university or institution for the award of a diploma, or degree at any level. Duly other works and/or researches cited in this work have been acknowledged under references.

……	…….
Abrokwa Aboagye Sintim	Prof. Augustine Kwame Kyere
(Student)	(Principal Supervisor)
Date……	Date…….
……	…….
Dr Francis Hasford	Mr. Kwabla Edem Sosu
(Co-Supervisor)	(Co-Supervisor)
Date……	Date……

ABSTRACT

Weighted and average dose within a scan volume of a phantom have been evaluated and validated using two different devices and techniques. The Barracuda electrometer and Ion Chamber techniques were applied on a 16 slice Siemens CT scanner and the results compared to the console displayed $CTDI_w$ and $CTDI_{vol}$ valuesfor accuracy and compared to each other for validation purposes. With fixed exposure parameter of 130kVp and varying tube current-time products from 140mAs to 300mAs for the CT head phantom examination, there were varying deviations in both the $CTDI_w$ and $CTDI_{vol}$ from the two techniques. Tube currents of 140 mAs, 240 mAs and 300 mAs yielded 3.5%, 0.61% and -6.45% deviations when the respective $CTDI_{vol}$ values for both techniques were compared. There were mean $CTDI_{vol}$ of (42.3 $\pm$ 8.6) mGy and (42.1 $\pm$ 8.1) mGy for Barracuda and Ion Chamber techniques respectively with an average deviation of 1.4 mGy between them, when the tube current-time products were varied from 140 – 300 mAs for the head phantom examination. Tube current-time products ranging from 80mAs – 220mAs were used for the CT body phantom examination and mean $CTDI_w$ measured were (16.6 $\pm$ 6.7) mGy and (16.5 $\pm$ 7.7) mGy for Barracuda and Ion Chamber techniques respectively with an average deviation of 1.0 mGy between them.

The estimated head and body dose deviations were compared to international dose accuracy range. The results of the study showed that the deviations from the techniques were within a range of $CTDI_w$ and $CTDI_{vol}$ values which were favorably comparable to other similar retrospective research works, thus, the Ion Chamber technique can be used in place of the technique currently in use.

DEDICATION

To my parents, Mr. Isaac Ansah Ampofo and Mrs. Faustina Amoaba whose support and guidance have gotten me another milestone in life.

ACKNOWLEDGEMENTS

My weighty thanks to God Almighty for His abundant grace and mercies on me throughout my study and providing me with all I needed during this research work.

I am very grateful to my indefatigable supervisors, Prof. Augustine Kwame Kyere, Dr. Francis Hasford and Mr. Edem Sosu for their guidance, encouragement and educative comments during the entire research process. I am indebted to my supervisors, their encouragements, criticisms and motivational words have contributed in bringing the research work this far.

My heartfelt gratitude goes to Mr. George Felix Acquah and Mr. Philip Oppong Kyereme Jnr. of Sweden Ghana Medical Centre (SGMC) who were there to assist and provide the needed materials for this research work. Special thanks to the medical physicists at Radiological and Medical Sciences Research Institute (RAMSRI) of Ghana Atomic Energy Commission (GAEC) for helping with the procedures involved in the use of the PTW pencil Ion Chamber.

My dearest thanks to my parents, Mr. Isaac Ansah Ampofo and Mrs. Faustina Amoaba, for their unending love and continual support. My friends Otu Asare, Rexford Atakora, Comfort Mirekua, Bedwei Hadeje, Daniel Osei and colleagues of 2016 medical physics class especially Daniel Ackom and Linus Owusu-Agyapong, may God bless all and sundry for your good company throughout our studies.

TABLE OF CONTENTS

LIST OF TABLES

LIST OF FIQURES

LIST OF PLATES

LIST OF ABBREVIATIONS

AAPM	American Association of Physicists in Medicine
ALARA	As Low As Reasonably Achievable
C (unit)	Coulombs
CAT	Computed Axial Tomography
CT	Computed Tomography
CTDI	Computed Tomography Dose Index
$CTDI_{100}$	Computed Tomgraphy Dose Index measured over 100mm pencil Ion Chamber
$CTDI_{FDA}$	Computed Tomography Dose Index defined by US Food and Drug Administration
$CTDI_{vol}$	Volume Computed Tomography Dose Index
$CTDI_{w}$	Weighted Computed Tomgraphy Dose Index
DLP	Dose – Length Product
DRLs	Diagnostic Reference Levels
EPT	Electronic Beam Tomography
FOV	Field of View
GAEC	Ghana Atomic Energy Commission
IAEA	International Atomic Energy Agency
ICRP	International Commission on Radiological Protection
ISD	Inter-scan Delay

mAs	milli ampere second
MDA	Multiple Computed Detector Arrays
MDCT	Multi Detector Computed Tomography
mGy	milli Gray
MRI	Magnetic Resonance Imaging
MSAD	Multiple Scan Average Dose
MSCT	Multi-Slice Computed Tomography
NRPB	National Radiological Protection Board
P1	Peripheral one
P2	Peripheral two
P3	Peripheral three
P4	Peripheral four
RAMSRI	Radiological and Medical Sciences Research Institute
SGMC	Sweden Ghana Medical Center
SSCT	Single Slice Computed Tomography
TLDs	Thermoluminesence Dosimeters
X-ray CT	X-ray Computed Tomography

CHAPTER ONE

1 INTRODUCTION

1.1 Overview

This chapter provides a general overview of the background as well as the research problem of the study. There are also discussions on research objective, scope and limitations. This section ends with discussion on the justification of the research work and organization of the study.

1.2 Background

Computed Tomography (CT) is a procedure that uses special x-rays equipment to create detailed slices of images. CT is an important imaging tool that is used in radiological diagnosis procedure with faster acquisition time compared to other imaging scanners, like Magnetic Resonance Imaging (MRI). CT examination involves the use of ionizing radiation. (Lechel et al., 2009) reported that, CT examination is asssociated with higher radiation exposures and can be seen in Appendix A. Different CT scanners have different number of slices that can be scanned and increasing the slice number increases the collective radiation dose. In 2007, Brenner & Hall reported on concerns of radiation dose to patients and the possibility of cancer occurrence. Increasing incidents of radiation overexposure in CT examinations has led to the interest of evaluating radiation doses in CT (UNSCEAR, 2013).

CT procedures consist of exposures from multiple rotation of the radiation source and the total dose to the irradiated volume is the accumulated dose from the adjacent scans (Bauhs et al., 2008). Multiple scan average dose (MSAD) is one name used for the accumulated dose; it is the dose from a multiple scan examination that is averaged over a single scan interval in the central portion of the multiple-scan dose profile (Bauhs et al., 2008). Thermoluminescent dosimeters (TLDs) or film are used in

measuring MSAD but both require considerable time for the measurement due mainly to the difficulty in calibration, reading and handling.

(Shope et al., 1981), introduced the idea of Computed Tomography Dose Index (CTDI) which they defined as the integral of the single scan radiation dose profile along the z-axis that is normalized to the thickness of the imaged section. With corrections to scan spacing, they showed that CTDI can estimate MSAD in a standardized and convinient manner. CTDI is a volume-averaged measure (AAPM, 2008; Bauhs et al., 2008).

CTDI can be measured using a 100-mm long pencil ionizatIon Chamber and denoted $CTDI_{100}$ (AAPM, 2011). The ionizatIon Chamber is placed in the CT head and body phantom and the CTDI is measured in the axial scan mode for an individual rotation of the x-ray source. Measurements of dose are taken at the center and at the periphery of the phantom and combined using a weighted average ($CTDI_w$) to give a single estimate of the radiation dose to the phantom. $CTDI_{vol}$ represents radiation output from the CT scanner to the phantom; $CTDI_{vol}$ measured in the CT head phantom is a reference to head CT and pediatric body CT in some cases and $CTDI_{vol}$ measured in CT body phantom is used as a reference to adult CT in the body (chest, abdomen and pelvis) and can as well serves as a reference to the pediatric body CT (Shrimpton, 2004).

1.3 Statement of Problem

In the event when a screen-film is exposed to too much radiation, there is a visual indication of excessive patient dose on the film. Unlike screen-film, CT images never look overexposed, as the modality provides image of normalized tissue attenuation values with often better image if excessive radiation is used. In computed and digital radiography which has a similar case to CT, overexposure will reduce image noise and mostly happen without the awareness of the operator, as radiologists do

not often care about image noise being too low (Bauhs et al., 2008). Hence, without dose measurements, the CT operator or user lacks the visual indications that are required to correctly adjust the tube potential or tube current-time product in avoidance of excessive patient dose.

Currently in Ghana, the available means of measuring the CT dose is by the use of the Barracuda which automatically estimate the CTDI values when the specified tube potential and tube current-time product are entered in the system. The Barracuda technique has been in use for quite some time in Ghana now.

With the acquisition of a new PTW Ion Chamber and electrometer by Ghana Atomic Energy Commission (GAEC), there is the need to therefore assess and validate the CTDI values obtained from the Barracuda equipment. The new equipment obtained by GAEC records charges during CT procedure and with the use of formalisms from the American Association of Physicists (AAPM) in Medicine Report 96 in 2008, the charges can be converted to exposure and subsequently to dose in air. This validation is needed to give an indication of whether or not the CTDI values obtained from the Barracuda and the new technique falls within the acceptable ranges and whether or not either one can be used in the absence of the other. To our knowledge in Ghana, there has not been any study to validate the CTDI values obtained by using the Barracuda equipment due mainly to lack of alternative device and technique. It is therefore pertinent to assess and validate CTDI values by using these two different techniques.

1.4 Objectives

The main objective of the research is to evaluate and compare the CTDI values obtained by the widely used Barracuda equipment in Ghana and the Ion Chamber technique obtained by GAEC for the

estimation of radiation dose during CT examinations when both techniques are subjected to the same conditions.

1.4.1 Specific objectives

- To evaluate CTDI values using Barracuda electrometer in Sweden Ghana Medical Center (SGMC).
- To evaluate CTDI using the PTW pencil Ion Chamber technique obtained by GAEC
- To compare the CTDI values obtained from the widely used Barracuda technique in Ghana with that obtained from the Ion Chamber technique from GAEC.
- To compare the CTDI values from both device and techniques to some international diagnostic reference levels (DRLs).
- To make appropriate recommendations if any from the results of the study.

1.5 Relevance and Justification

This work would be helpful in the optimization of patients' protection during CT procedures in Ghana specifically at Sweden Ghana Medical Center. From literature, CT gives a significant portion of effective radiation dose to patients, even though, it represents only a small portion of all radiologic procedures (Brix et al., 2009; Brenner & Hall, 2008; Mettler et al., 2000). There is the worrying issue of higher radiation dose in CT as compared to other imaging procedures to medical practitioners and scientific researchers. With the continual use of CT in the diagnostic field and the advancement in the technology, the issue of higher radiation dose is still of great concern. There is the need to therefore measure the amount of radiation dose given to patients during CT examinations with CT dosimetry measuring devices and techniques. Unfortunately, there is one device and technique in quantifying

radiation dose in Ghana during CT examinations. This study is therefore to use a different device and technique to validate the results obtained from the existing technique in the estimation of radiation dose to patients during CT procedures to enhance the degree of confidence in the existing technique. There is also the need to assess the limitations in the use of CTDI as the means of estimating radiation dose to patients in CT examinations.

1.6 Scope and Delimitation

The study is primarily focused on the estimation of radiation dose from CT examinations at Sweden Ghana Medical Center using Barracuda technique in calculating CTDI values and PTW Ion Chamber connected to electrometer that records charges from CT procedures. The dose measurements were made using cylindrical CT dosimetry phantoms; head phantom (16-cm in diameter) and body phantom (32-cm in diameter). Normalized conversion factors based on body specific anatomy and dose-length product (DLP) values were used in the Barracuda for the dose estimations. In the PTW Ion Chamber and electrometer technique, mathematical equations and AAPM Report 96 formalisms were employed in the dose calculations after the charges had been recorded.

1.7 Structure of the Thesis

The organization of the thesis is as follows: Chapter one gives the background of the thesis as well as the statement of the problem and the objectives for the study. Chapter two presents the existing literature relevant to this study. The materials used and procedure employed in obtaining the research findings is presented in chapter three. The analysis of research findings and discussion is presented in chapter four. Lastly, chapter five recaps the study by presenting the conclusions and recommendations for further study.

CHAPTER TWO

2 LITERATURE REVIEW

2.1 Overview

This chapter provides detailed background regarding basic knowledge in CT and CT dosimetry. The chapter also contains details for principles of CT scanners and relevant literature pertinent to the research study.

2.2 Introduction

Computed tomography (CT) also known as computed axial tomography (CAT) was invented and introduced into clinical use in the 1970s. By then, it was considered as the most advanced machine since the development of x-ray machine (Goergen et al., 2009). Beam width has increased significantly from a standard of 10 mm to current beam widths of up to 160 mm. The use of CT has been increasing rapidly; there have been 12-fold and 20-fold increases in CT in European countries and the United States over the last 20 years (Hall & Brenner, 2008). CT scanners start to take a center stage in the imaging world with the introduction of single detector CT scanner that takes an image one at a time, with the x-ray tube and detector rotating 360 degrees or less and the patient and table staying fixed (Seeram, 2009). This cross-sectional imaging modality supplies diagnostic radiology with better visualization into the pathogenesis of the body, exhibiting smaller contrast differences than conventional x-ray images and increasing the chances of recovery.

From the early part of 1990s until present, CT ability to acquire multiple slice at a time has led CT scans to be one of the most important methods of radiological diagnosis (Siemens, 2010). The number of slices range from 4, 6, to 64 and up to 320 for the more modern CT scanner machines. This is

normally referred to as multi-slice (MSCT) or multi-detector (MDCT) technology (Marchal et al., 2005). The techniques and procedures of CT have been expanded in the past few years, leading to an increase in the use this imaging modality and similarly the radiation dose to the patient and concern surrounding this has also increased. CT scanning is capable of providing high quality images that are valuable for adequate diagnostic information, however it is also described and perceive as a high dose procedure (Kulama, 2004). During a CT examination, the radiation dose imparted to the patient can be high, for that matter it is important to keep the radiation exposure as low as possible, paying much attention to the image in order to maintain a clear image quality that is suitable for diagnostic task (Jurik el al., 1997)

It is well-known that CT delivers high radiation doses compared with other imaging modalities that uses x-ray applications. Various authors have reported altered dose values for a CT examination of an identical region. Variations in scan protocols mean that several units of dose measurement are used; thus, correlation of CT with other radiological procedures can be difficult, and this has delayed comparisons between studies. With a mean effective dose ranging from 1 mSv to 5 mSv, about 30 to 40 percent of all CT studies are surveys of the head or brain in clinical practice (Mulkens et al., 2007).

Many international associations have set guidelines to regulate CT examination in order to reduced radiation dose delivered to patients. The European guidelines comprise image quality criteria for most CT examinations, high-quality imaging procedures and the use of Diagnostic Reference Levels (DRL) (Tsapaki & Rehani, 2007). DRL is aid at setting dose levels in different CT examinations and allow assessment to be made between different scanners and techniques, and make it easy for comparison. All of this helps in improving patient protection by reducing the patient dose while maintain image quality and providing advice to use and select the right dose for a particular CT examination. In the United States of America, it is estimated that CT scanning accounts for more than 10% of all

radiological examinations, while the radiation dose to the patients connected with medical imaging is about 75% (Tsapaki & Rehani, 2007).

In 1999 the National Radiological Protection Board (NRPB) conducted a survey that showed 4% of all diagnostic examination is CT, which accounts for about 40% of the patient dose. Previously in 1990, the collective effective dose from medical exposure to the population was 20% (Kulama, 2004). In the UK, CT accounts for 5% of the radiological examinations, however it added about 34% to the collective dose of radiation exposure (UNSCEAR, 2000). The increasing use of CT facilities raises concern about the radiation dose to patients and workers. Due to this, continuous efforts should be made in the area of decreasing doses to staff and the population. There are many methods used for the optimization of patient dose whiles maintaining image quality good enough for diagnosis (Aweda & Arogundade, 2007).The use different models of CT scanners, vary the radiation dose to the patients substantially due to varying CT geometry and filtration. Evidence have showed that the image quality acquired from CT scanners is much higher than really necessary to produce precise clinical diagnosis (Tsapaki & Rehani, 2007).

Thus, CT manufacturers, radiologists and physicists together should put measures in place for decreasing patient dose, and expand and develop CT scanners to provide the needed image quality with low radiation dose to the population (Kalra et al., 2004). If CT examination is clinically acceptable, justified and doses remain optimized then CT can be a very useful tool. While the use of CT scanners has increased recently, the effect of radiation doses to patients has also increased and this has raised concerns for needing to decrease radiation exposure from CT scanners. The radiology society has applied CT dose reduction applications that match the standard of as low as reasonably achievable (ALARA) in response to the growing awareness from the population ((McCollough et al., 2009).

Due to this public awareness, dose reduction has become a major concern in the use of CT. Because of inadequate guidelines and a limited research foundation on the topic of CT examination and scanning techniques, different methods have been used towards optimizing of radiation dose (Kulama, 2004). The rapid development of MSCT scanners and the increasing number of CT scan examinations, corresponding to the large amount of radiation dose collected from all medical procedures, have enhanced these worries. Other concerns raise about MSCT imaging is the inappropriate use of CT scanners, for example scanning the area away from region of interest. There are other factors affecting radiation doses to patient, such as radiologist and technologist chosen parameters including tube current-time products (mAs), and tube potential (kVp) and differences in scanning parameters; all of these factors have a major effect on the patient dose.

Rehani and Berry in 2000 pointed out that, computed tomography tests are hazardous and that there should be a guarantee that the examinations asked for are justified and most suitable for patient need and diagnosis. This is to ensure a decrease in patient exposure and in compliance to the recommendations of the International Commission on Radiological Protection (ICRP) which advises that all exposures should be as low as reasonably achievable (ALARA) (Catalano et al., 2007). The major dose reduction tool in radiation protection is the process of proper justification of a study, that is, the avoidance of pointless procedures. However, where an examination is undertaken, the importance must be on dose optimization; attaining the required image quality at the smallest possible dose level. This can be reached in two ways: the first is during the design of dose efficient equipment, and the second is via the optimization of scan protocols (Lewis & Edyvean, 2005).

2.3 Principles of Computed Tomography (CT)

A CT scan, also called X-ray computed tomography (X-ray CT) or computerized axial tomography scan (CAT scan) makes use of computer-processed combinations of many x-ray images taken from different angles to produce cross-sectional tomographic images (virtual 'slices') of specific areas of a scanned object, allowing the user to see inside the object without cutting. The CT scanner is a machine that uses on an x-ray source which when applied gives an accurate information on the attenuation possessions of a thin sectional volume of the body, which will be absorbed at different levels and produce a matrix or profile of x-ray beams of the same strength. The basic elements of CT are the high capacity x-ray tube source, which rotates around the patient and generates an x-ray beam, a rotational geometry with respect to the object being imaged and the x-ray detector recording the radiation that crosses the body (Hanafi, 2005).

2.4 Evolution of CT scanning

Historically, CT scanners has undergone a series of transformation from generation to generation. CT scanner generation starts with pencil- thin beam, to small fan, to fan beam with rotating detector, and fan beam with stationary detector (Kalender, 2005). The differentiable feature among different scanners is the detector width and the gantry opening size. Today, the general scanner design for clinical CT appears standardized to some level. A number of dedicated scanners using flat-detector technology are on the increased such as dedicated scanners for the breast, for the faciomaxillary skull and the extremities as well as the use of C-arm–based scanning for interventional and intraoperative imaging using flat detectors is also showing some increase.

2.4.1 First Generation CT Scanners

The first CT scanner was developed in the early 1970s by Hounsfield, a computer engineer in England (Kalender, 2005). The first generation of CT scanners utilizes a pencil beam x-ray source position at a fixed source interval with only one detector acquired image data by a 'translate-rotate' method. The combination of the x-ray tube and detector moved in a linear motion across the patient (translate) and this system motion was repeated until the beam and detector reached 180 degrees. When the x-rays were emitted from the source and penetrated through the patients, the intensity of x-rays was evaluated from a sequence of transmission measurements made by the detector. This process is repeated for an acquisition of 180 projections at one-degree interval surrounding the patient generating 28,800 x-ray of total measurements. From these measurements, an image was created. The first generation CT scanners projected a succession of parallel beams at different locations through the patient as it's translate linearly across a specific field of view (FOV). When the system has completed the appropriate field of view for a particular accusation, it rotates one degree and the translation process is repeated in the following projection(Bushberg et al., 2011a)

One advantage of the first-generation CT scanner was that it employed pencil beam geometry-only two detectors measured the transmission of x-rays through the patient. The pencil beam allowed very efficient scatter reduction, because scatter that was deflected away from the pencil ray was not measured by a detector. With regard to scatter rejection, the pencil beam geometry used in first-generation CT scanners was the best (Bushberg et al, 2011b). However, the disadvantage of these scanners was the scan time, which took approximately 4 - 5.5 minutes to produce an image, and the limitation of the device to the head only (Cunningham & Judy, 2000). Figure 2.1 shows the first-generation CT scanner, which used a parallel x-ray beam with translate-rotate motion to acquire data

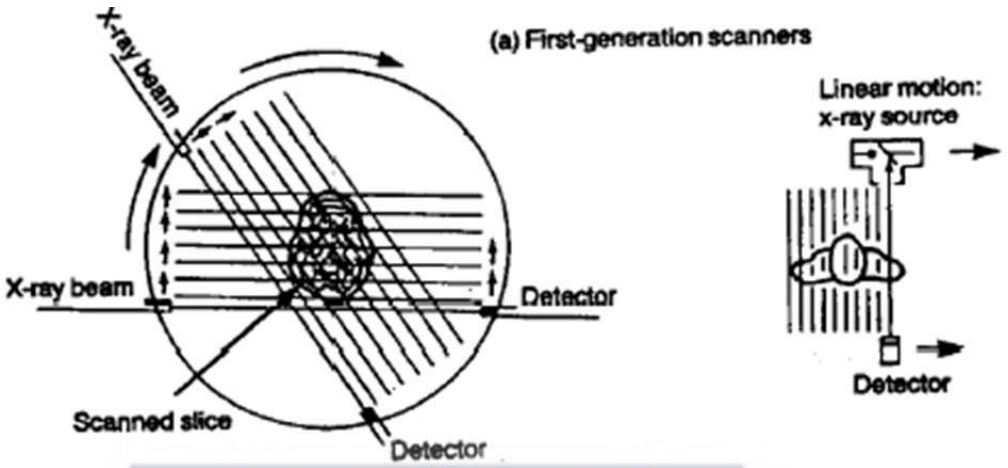

Figure 2.1: Schematic diagram of the first-generation CT scanner

2.4.2 Second Generation CT scanner

The second generation of the CT was introduced in 1972 for purpose of improving image quality and scan time. The x-ray source was changed from the pencil beam to a narrow fan shaped beam geometry (10 to 15 degrees) together with multiple detectors. These scanners decreased the scan time and improved the image quality, but increased the amount of scatter radiation (Carlton, Adler, & Bushong, 2005). With improvement made from first to second generation CT scanners, the average scan time was reduced from few minutes to few tens of seconds. The angle of rotation between the translation motions increase considerably as a result of the narrow fan beam and multiple array of detector system used.

Data analysis and processing efficiency was improved per rotation through the multi detector system, minimizing the total number of revolution required to produce an image and the increase in detector number from 2 to 30 improve the x-ray beam use to produce the image. The clinical used of the first and the second generation CT scanners were only restricted to head scan protocols due to prolong image acquisition time. However, with the improvement made on the second generation CT scanners, a few body scans were executed. Figure 2.2 below shows the second-generation CT scanner, which

used translate-rotate motion to acquire data.

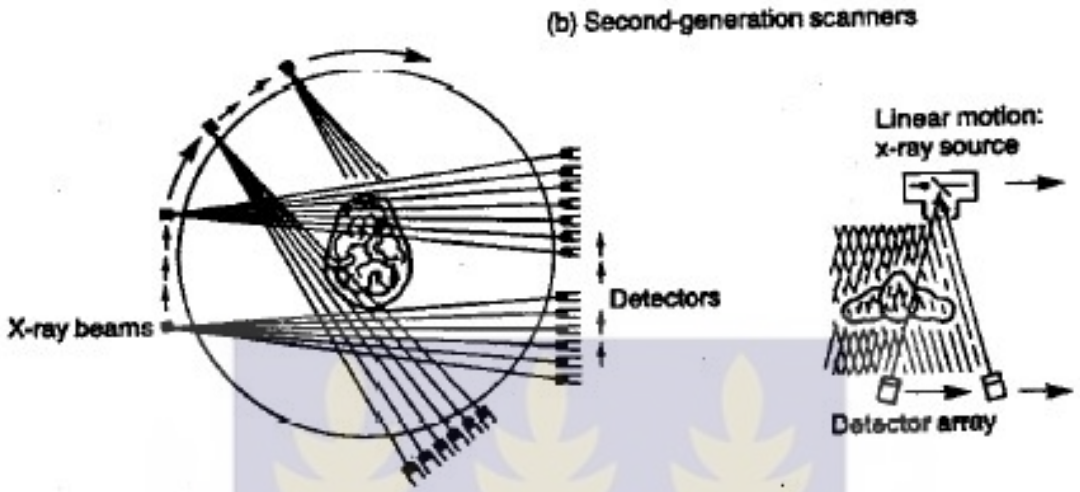

Figure 2.2: Schematic diagram of the second-generation CT scanner

2.4.3 Third Generation CT Scanner

The number of detectors used in third-generation scanners was increased substantially, and the angle of the fan beam was also increased so that, the detector array formed an arc wide enough to allow the x-ray beam to interact with the entire patient. Third generation CT scanners saw the evolution of elements of the modern CT scan, which uses a wide fan shaped beam and a curved detector array with up to 750 detectors. The wide fan beam was wide enough to include the whole patient in an individual exposure. These scanners decreased the scan-time to nearly 1 second for a single image and improved the image quality, but the use of a moving detector created a problem called a 'ring artefact' (Carlton et al., 2005). Figure 2.3 below shows the third-generation CT scanner, which acquires data by rotating both the x-ray source with a wide fan beam geometry and the detectors around the patient.

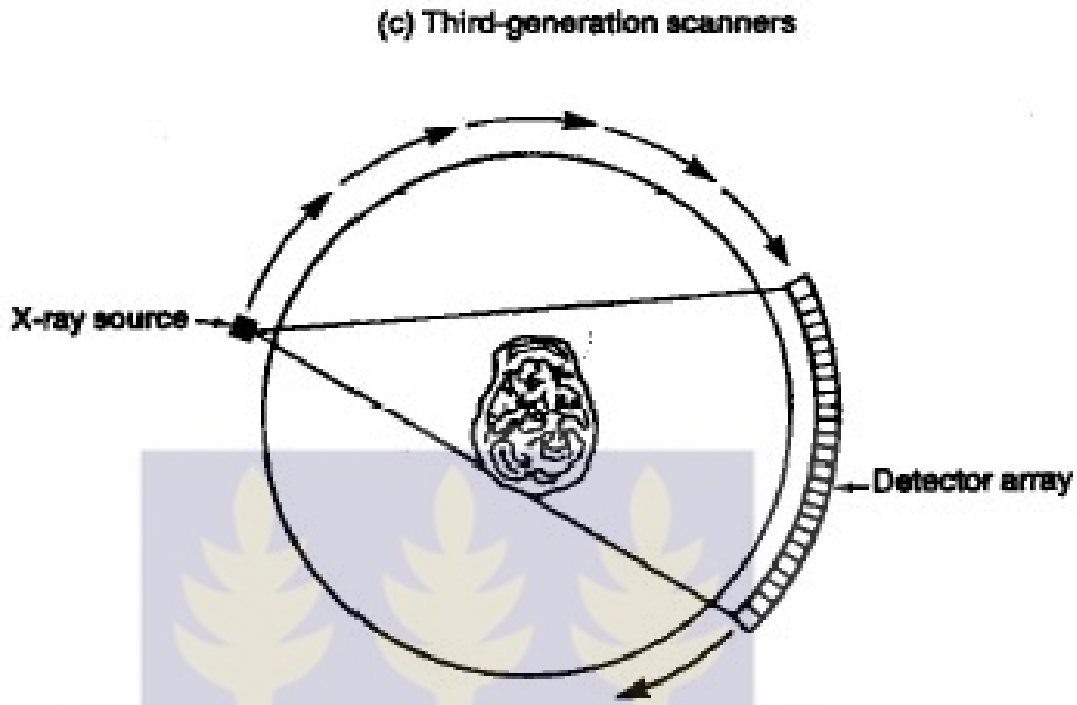

Figure 2.3: Schematic diagram of the third-generation CT scanner

2.4.4 Fourth Generation CT scanner

Fourth-generation CT scanners were designed to overcome the problem of ring artifacts. With this CT scanners, the detectors are removed from the rotating gantry and are placed in a stationary 360-degree ring around the patient, requiring many more detectors. Modern fourth-generation CT systems use about 4,800 individual detectors. Because the x-ray tube rotates and the detectors are stationary, fourth-generation CT is said to use a rotate/stationary geometry. The design was based on a rotating x-ray source and stationary detector and achieved scan-time ranges from 2 to 10 seconds (Carlton et al., 2005). Figure 2.4 below shows the fourth-generation CT scanner, which uses a stationary ring of detectors positioned around the patient.

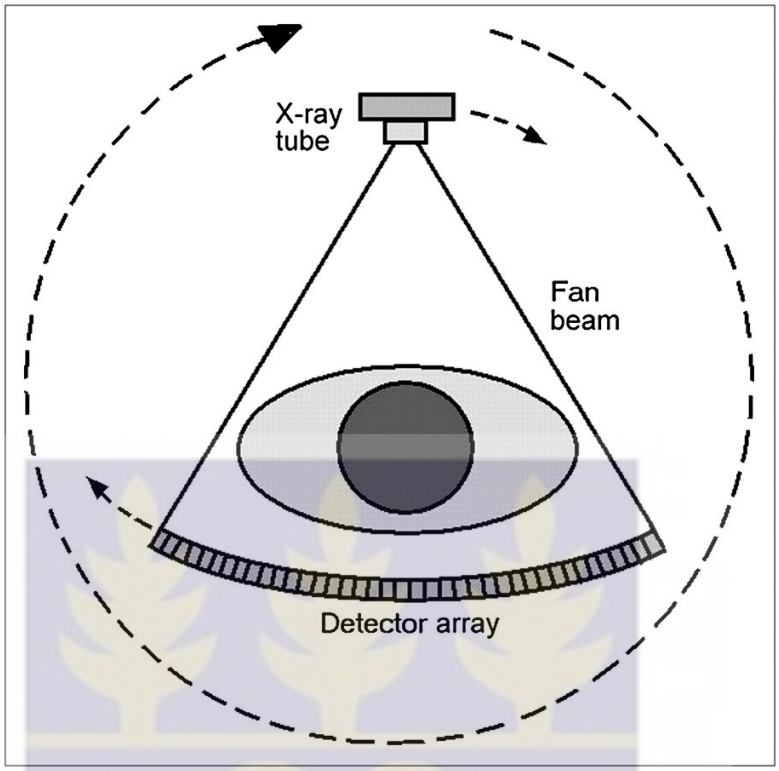

Figure 2.4: Schematic diagram of the fourth-generation CT scanner

2.4.5 Fifth Generation CT scanner

This generation of scanners is referred as cardiac cine CT or Electronic Beam Tomography (EPT). The parts in these systems are stationary for which; the x-ray source and detectors are both fixed. These group of scanners from that of the conventional x-ray tube, but consist of a large semi-circle ring that surrounds the patient, allowing high speed CT scanning to acquire 17 images per second (Carlton et al., 2005; GE Health care, 2003).

2.4.6 Sixth Generation CT scanner

This generation of scanners, also known as Helical/Spiral CT, uses slip ring technology, where many images are acquired while the patient is transformed through the gantry (Fishman & Jeffrey, 1998).

Normally in helical CT, the x-ray tube is continuously rotating while the table (couch) is fixed during the examination, allowing patient images to be acquired within one single breath hold (Cunningham & Judy, 2000). The design of slip ring technology comprises of many sets of matching rings to allow the current and voltage to the x-ray tube, without cables connecting directly to the tube. This avoids the x-ray tube from stopping during its continuous rotation. The main advantages of these scanners include the shorter scan time, avoiding overlap and reduction in the motion 'artefact' (Carlton et al., 2005).

2.4.7 Seventh Generation

In this generation, CT scanning improved with the introduction of multiple detectors and has been referred to as Multi detector Computed Tomography (MDCT), Multi-slice Computed Tomography (MSCT) and Multiple Computed Detector Arrays (MDA) (Carlton et al., 2005). The main feature of these scanners is the number of detectors, which varies from two to 320 rows of detectors (Katada, 2002). The number of detectors impacts on the total time of examinations for the body and chest being completed in 15 to 20 seconds.

2.4.8 Helical /Spiral CT

Technological development has seen the introduction of helical CT in the early 1990s which led to good image quality and faster scan times; this is considered as a major advancement in CT scanning (Cunningham & Judy, 2000). Helical CT utilizes slip-ring technology to acquire data continuously as the patient is translated through the gantry (Fishman & Jeffrey, 1998). The Slip rings are electro-mechanical devices consist of a sets of parallel conductive rings concentric to the gantry axis which connect to the x-ray tube, detectors and control circuit by sliding contactors. By using slip-ring

technology in spiral CT, the gantry performs multiple 360º rotations constantly while the patient is moved continuously through the scan field in the z-direction through the gantry during the scanning and data acquisition process. This technique eliminates the need for the cables that supply the kVp and mAs to the tube, which would otherwise have to be rewound between scans (Cunningham & Judy, 2000). The helical CT is referred to as volume scanning. The major advance in helical CT in comparison to earlier machines is the faster scan time, taking just a minute to complete an abdomen and chest scan which can be done in a single breath-hold. Also it reduction in patient movement during exam and is ideal for three-dimensional imaging (Fishman & Jeffrey, 1998).

2.4.9 Conventional CT

conventional CT have been developed from the concept of third CT generation where the x-ray tube rotates round the patient to collect the patient data providing one slice in each gantry rotation (Seeram, 2009). In Conventional CT, scanning requires a rotating x-ray tube to collect patient data, providing one slice in each gantry rotation (Seeram, 2009). During the procedure, the patient is required to stay still without moving (Michael, 2001). The rotation of the x-ray tube in conventional CT scanners is limited by cables, which supply the milliampere (mA) and peak kilovoltage (kVp). The image acquisition mode in conventional CT is axial and cluster scanning, which is designed to collect numerous slices from one patient within a second, and is attainable via an active scanning sequence. Every cluster is known as a group (GE Healthcare, 2003).

In conventional CT, the x-ray tube should be accelerated to a steady speed of rotation while the cable should be extended enough to permit an entire 360-degree rotation (Seeram, 2009). To avoid intertwining the cable, the tube detector is required to change direction in each scan. Therefore, when the cable goes back to the normal position, a stoppage will occur between each scan attainment called interscan delay (ISD) (GE Healthcare, 2003). While the x-ray tube rotates, the generated x-rays pass

through the body to drop on the detectors to determine the virtual diffusion value. While the tube is rotating, the patient holds a breath (Seeram, 2009), although the patient is able to breathe normally during the ISD time. It is essential for the patient to hold their breath during the scan, despite the fact that the aim is to reduce motion during the examination of the chest and abdomen (GE Healthcare, 2003). Using a conventional CT, a single image can be achieved in around 0.5 seconds and the whole exam may produce 20 to 30 images that only take minutes to be completed (Michael, 2001).

conventional CT scanners has come with many limitations which are mostly related to the scan time during the stop and shoot mode, and the importance for the patient to breathe during the examination, which increases the ISD time. Furthermore, patient's breath-hold may not be steady during the exam which may leads to loss of anatomic region in the scan. In addition to this, not many images are taken when the contrast media technique is applied (Seeram, 2009). This has therefore call on more effort to improve the conventional CT scanner in order to overcome these limitations, which has led to the development of the spiral CT.

2.5 Multi-Slice CT

Multi-slice CT (MSCT) also known as multi row CT or multi detector row CT (MDCT) has been introduced in to the imaging realm by Elscint since 1992 (Kalender 2005). MSCT is a CT system designed with multiple rows of CT detectors, combined with helical/spiral scanning to produce images made up of multiple slices. MSCT has noticeably enhanced the performance of CT in terms of image resolution, production of thinner sections and a reduction in the time taken for examinations. Recently, the multi-slice CT systems appears with two, four, eight, 16, 32 and 64 detectors, and more recently a 320 row system (Katada, 2002). Radiation doses associated with a 64-slice CT was investigated by Fujii et al. (2009) in phantom study. Their study showed that a 64-slice CT provides the same organ

and effective doses for adults and children, similar to those with 4, 8 and 16-slice CT scanners, which gives an indication of high doses from MSCT scanners (Fujii et al., 2009).

2.6 Principle of MSCT

In MSCT scanning, the x-ray tube is a rotary anode with a high heat aptitude, the beam is fan shaped and originates from either a small or large focal spot. The tube supplies kVp ranges from 80-140 and a mAs of 10 - 500 (Seeram, 2009). Detectors in MSCT are the main features and are in to three detector types (Katada, 2002). First detector is the matrix detectors, which involve several detector rows, each of matching depth; then the second type of detector is the hybrid detectors, which are similar to the matrix detectors except the outer rows are wider than the deepest one in the hybrid detectors; and thirdly, the adaptive array, in which the rows have different widths, which means that the rows increase in thickness from the core of the slice to the marginal area (Marchal & Heiken, 2005).

MSCT allows the operator to choose a variable slice thickness, similar to or larger than the set slice thickness. To gain optimal spatial resolution, the acquired slice thickness should be small, and indeed the smaller the slice thickness, the better the sampling along the z-axis. Using this method of reconstruction allows the MSCT scanner to obtain the sagittal and coronal planes without requiring a particular positioning procedures (Kulama, 2004). Quite a number of features have improved the utility of MSCT in three dimensional imaging identification and analysis using computer graphics. This has provided the MSCT with a high level of precision, which has allowed it to visualize very small details which could not be attained with other types of CT scans (Katada, 2002). While a very thin slice of 1 or 0.5 mm can be used in MSCT, mAs are generally increased to maintain very low noise in the imager and keep the image quality high, and the patient dose is also increased. The main diagnostic advancements in CT is the improvement in image quality with less

signal to noise ratio and high contrast resolution with no artefacts. However, these are not the only parameters as the dose to the patient and examination time also important considerations (Kulama, 2004). Additionally, there are many parameters which can affect the image quality such as slice thickness, pitch, and radiation dose, low and high contrast resolution and noise. These all differ depending on the companies and the scanner model being used.

Multi-slice CT with better image quality is obtained with known pitch taken into consideration, as the pitch is directly linked with image quality and exposure dose. Generally, to enhance image quality, the dose to the patient is increased; but if the pitch is increased, the image quality is reduced, and the dose is also reduced (Katada, 2002). Of late, limiting the radiation dose to the patient with decrease image quality has been the main concern and nonetheless, a balance between dose and image quality needs to be achieved (Kulama, 2004).

2.6.1 MSCT Detector

The detector system in MSCT is different from single slice CT (SSCT) in terms of the detector configuration. MSCT detectors are in an array, segmented in the z axis which means there are more rows of detectors next to each other allowing for simultaneous acquisition of multiple images in the scan plane with one rotation (Goldman, 2008; Bongartz et al., 2004). In 2002, 16-slice CT scanners was introduced in to the medical world, providing 16 data channels to obtain 16 slices in one rotation. In 16-slice CT, the detectors are joined together to allow smaller slices to be obtained. This design works because the innermost 16 detectors are half the size of the external elements, allowing the attainment of 16 thin slices that range from 0.5 - 0.75 mm thick. MSCT companies started to introduce 16-slice and 8-slice models in 2003 and 2004. Around the same time, 32-slice and 40-slice scanners were being introduced.

In 2005, 64-slice scanners were introduced, with different companies using different designs for the

detector array. They use a periodic motion of the focal spot in the longitudinal direction (z-flying focal spot) to double the number of simultaneously acquired slices. Each of the 32 detectors collects two measurements separated by 0.3 mm, therefore the net result gives a total of 64 slices (Goldman, 2008). Today, modern CT scanners are capable of imaging simultaneously 128 or even 320 parallel slices in one rotation (Geleijns et al., 2009). Beam width has increased significantly from a standard of 10 mm to current beam widths of up to 160 mm. figure 2.5 shows detector array configurations of some manufacturers.

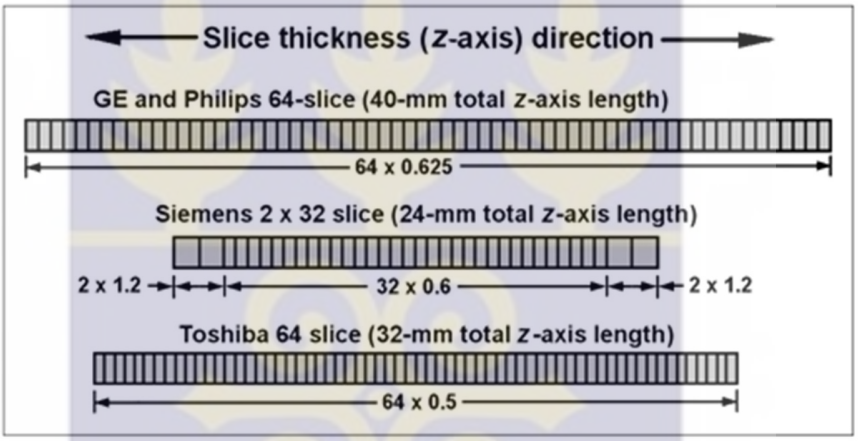

Figure 2.5: Diagrams of 64-slice detector designs in z-direction for different CT scanner manufacturers (Lee W. Goldman, 2008).

2.7 CT Dosimetry

With the introduction of the spiral CT in the early 1990s and subsequent introduction of four slice CT has revolutionaries modern CT scanning capable of providing high quality diagnostic information. This however, is generally describe as being a high dose procedure (Kulama, 2004). With 16 and 64 – slice CT scanners now available as well as models providing 320 slices with large area, have greatly change the clinical use of CT as new clinical applications have evolved. For instance, the use of vascular and cardiac exams, perfusion imaging and whole body imaging.

In CT imaging a number of factors affect the radiation dose delivered to patients. These includes; the

radiologist, application specialist and technician who choose the parameters for the tube current, tube potential (kVp) and the differences in scanning parameters (Catalono, et al., 2007). In MSCT examination, the radiation dose delivered to patients are quite high, this therefore call for the need to keep radiation as low as reasonable achievable (ALARA). Thus, extra careful is therefore needed to in reducing radiation dose and maintaining an image quality that is acceptable for diagnosis (Jurik et al., 1997).

The radiation dose to the patient will differ depending on the make and model of MSCT scanner in terms of variations in MSCT geometry, filtration and the awareness of the image quality from the CT scanner. This is where the needs are to be balanced between radiation dose and image quality (Tsapaki & Rehani, 2007).

It is necessary for manufacturers, radiologists, technologists and physicists to work together to find a plan to decrease patient dose (ALARA Principle). Advances in the use and development of MSCT scanners have resulted in the ability to provide images of adequate quality, with a resultant low radiation dose to the population (Kalra et al., 2004), however this is not commonly understood in the practical medical imaging field (Tsapaki & Rehani, 2007).

Many CT parameters have been briefly studied, and manufacturers have adopted an auto mA protocol for minimizing the radiation dose whiles keeping image quality constant. It is commonly believed that a change in the kVp is difficult, because any change in the kVp would have major impact on the image quality and dosage (McNitt-Gray & Geffen, 2006). The aim of optimization in diagnostic radiology is to achieve optimal parameters and protocols needed to create high image quality with the lowest possible dose to patients. As a result of this, optimization of radiation dose is necessary for each particular x-ray unit and for each x-ray examination. The optimization procedure requires an evaluation of patient dose and image quality (Mahesh, 2009).

2.7.1 Quantities for Assessing Dose in CT

2.7.1.1 Computed Tomography Dose Index (CTDI)

The primary dose measurement concept in CT is the CTDI and it represents the average absorbed dose, along the z-axis, from a sequence of contiguous irradiations. The CTDI is measured from one axial CT scan, and is calculated by dividing the integrated absorbed dose by the nominal total beam collimation (Jessen et al., 2000). The CTDI is continually measured in the axial scan mode for a single rotation of the X-ray source, and theoretically approximates the average dose within the central region of a scan volume consisting of multiple, contiguous CT scans [multiple scan average dose (MSAD)] for the case where the scan length is sufficient for the central dose to approach its asymptotic upper limit (Nagel, 2000). The MSAD represents the average dose over a small interval (- I/2, I/2) about the centre of the scan length (z = 0) for a scan interval I, but requires multiple exposures for its direct measurement. The CTDI offered a more convenient yet nominally equivalent method of estimating this value, and required only a single scan acquisition, which in the early days of CT saved a considerable amount of time.

$$CTDI = \frac{1}{NT}\int_{-\infty}^{\infty} D(z)dz \qquad (1)$$

Where,

D(z) = the absorbed dose profile along the axis of rotation of the scanner (z-axis),

N = the number of tomographic sections imaged in a single axial scan. This is equal to the number of data channels used in a particular scan. The value of N may be less than or equal to the maximum number of data channels available on the system, and

T = the width of the tomographic section along the z-axis imaged by one data channel. In multiple detector-row (multi-slice) CT scanners; several detector elements may be grouped together to form

one data channel. In single-detector-row (single-slice) CT, the z-axis collimation (T) is the nominal scan width.

2.7.1.2 $CTDI_{FDA}$

Hypothetically, the equivalence of the MSAD and the CTDI necessitates that all contributions from the tails of the radiation dose profile be included in the CTDI dose measurement. The exact integration limits required to meet this criterion depend upon the width of the nominal radiation beam and the scattering medium. To normalize CTDI measurements (infinity is not a likely measurement parameter), the FDA introduced the integration limits of ± 7T, where T represented the nominal slice width [United States FDA Code of Federal Regulations, 1984). Remarkably, the original CT scanner, the EMI Mark I, was a dual-detector row system. Hence, the nominal radiation beam width was equal to twice the nominal slice width (i.e. N x T mm). To account for this, the CTDI value must be normalised to 1/NT:

$$CTDI_{FDA} = \frac{1}{NT}\int_{-7T}^{7T} D(z)dz \qquad (2)$$

Unluckily, the limits of integration were not equally conveyed in terms of NT, permitting for the potential underestimation of the MSAD by the CTDI. For the technology available circa-1984, the use of NT in the integration limits was deemed unnecessary at the time (Dixon, 2006). The scattering media for CTDI measurements were also standardised by the FDA (United States FDA Code of Federal Regulations, 1984). These comprise of two polymethyl methacrylate (PMMA, e.g. acrylic or Lucite) cylinders of 14-cm length. To estimate dose values for head examinations, a diameter of 16 cm is to be used. To estimate dose values for body examination, a diameter of 32 cm is to be used. These are typically referred to, respectively, as the head and body CTDI phantoms.

2.7.1.3 $CTDI_{100}$

$CTDI_{100}$ represents the accumulated multiple scan dose at the center of a 100-mm scan and underestimates the accumulated dose for longer scan lengths. It is therefore lesser than the equilibrium dose or MSAD. The $CTDI_{100}$, like the $CTDI_{FDA}$, requires integration of the radiation dose profile from a single axial scan over specific integration limits. In the case of CTDI100, the integration limits are ± 50 mm, which corresponds to the 100 mm length of the commercially available "pencil" ionizatIon Chamber (AAPM, 1990; AAPM, 1993; McNitt-Gray, 2002).

$$CTDI_{100} = \frac{1}{NT}\int_{-50m}^{50mm} D(z)dz \qquad (3)$$

The use of a single, consistent integration limit avoided the problem of dose overestimation for narrow slice widths (e.g. < 3 mm) (AAPM, 1990). $CTDI_{100}$ is acquired using a 100-mm long, 3-cm3 active volume CT "pencil" ionizatIon Chamber and the two standard CTDI acrylic phantoms [head (16-cm diameter) and body (32-cm diameter)] (AAPM, 1990, United States FDA Code of Federal Regulations, 1984). The measurement must be performed with a stationary patient table. The pencil chamber of active length ℓ is not really measuring air kerma, but rather the integral of the single rotation dose profile D(z).

2.7.1.4 Weighted CTDI ($CTDI_w$)

The CTDI varies across the field-of-view. For example, for body CT imaging, the CTDI is typically a factor or two higher at the surface than at the centre of the field of view. The average CTDI across the field-of-view is estimated by the Weighted CTDI (CTDIw) (Jessen et al., 2000, International Electrotechnical Commission, 2002, Leitz et al., 1995), where

$$CTDI_w = \frac{1}{3}CTDI_{100,\ center} + \frac{2}{3}CTDI_{100,\ edge} \qquad (4)$$

The values of 1/3 and 2/3 approximate the relative areas represented by the centre and edge values (Leitz et al., 1995). CTDIw is a useful indicator of scanner radiation output for a specific kVp and mAs. According to IEC 60601-2-44, $CTDI_W$ must use $CTDI_{100}$ as described above and an f-factor for air (0.87 rad/R or 1.0 mGy/mGy) (Jessen et al., 2000, International Electrotechnical Commission, 2002).

2.7.1.5 Volume CTDI ($CTDI_{vol}$)

To represent dose for a specific scan protocol, which usually involves a series of scans, it is essential to take into account any gaps or overlaps between the X-ray beams from consecutive rotations of the X-ray source. This is accomplished with the use of a dose descriptor known as the Volume $CTDI_w$ ($CTDI_{vol.}$), where

$$CTDI_{vol.} = \frac{NT}{I} . CTDI_w \qquad (5)$$

I = the table increment per axial scan (mm) (International Electrotechnical Commission, 2002). Since pitch is defined (International Electrotechnical Commission, 2002) as the ratio of the table travel per rotation (I) to the total nominal beam width (N*T) (International Electrotechnical Commission, 2002, McCollough and Zink, 1999):

$$Pitch = \frac{I}{NT} \qquad (6)$$

Consequently, volume CTDI can be expressed as:

$$CTDI_{vol.} = \frac{1}{Pitch} . CTDI_w \qquad (7)$$

Whereas $CTDI_w$ represents the average absorbed radiation dose over the x and y directions at the centre of the scan from a series of axial scans where the scatter tails are negligible beyond the 100

mm integration limit, $CTDI_{vol.}$ represents the average absorbed radiation dose over the x, y and z directions. It is conceptually similar to the MSAD, but is standardized with respect to the integration limits (± 50 mm) and the f-factor used to convert the exposure or air kerma measurement into dose to air.

2.7.1.6 Dose-length product (DLP)

To better represent the overall energy delivered by a given scan protocol, the absorbed dose can be integrated along the scan length to compute the dose-length product (DLP) (Jessen et al., 2000), where

$$DLP\ (mGy\text{-}mm) = CTDI_{vol.}\ (mGy) \cdot \text{scan length}\ (mm) \qquad (8)$$

The DLP reflects the total energy absorbed (and thus the potential biological effect) attributable to the complete scan acquisition. Thus, an abdomen only CT exam might have the same $CTDI_{vol.}$ as an abdomen/pelvis CT exam, but the latter exam would have a greater DLP, proportional to the greater z-extent of the scan volume. In helical CT, data interpolation between two points must be performed for all projection angles. Thus, the images at the very beginning and end of a helical scan require data from z-axis projections beyond the defined "scan" boundaries (i.e. the beginning and end of the anatomic range over which images are desired). This increase in dose-length product due to the additional rotation(s) required for the helical interpolation algorithm is often referred to as over-ranging. For MDCT scanners, the number of additional rotations is strongly pitch dependent, with a typical increase in irradiation length of 1.5 times the total nominal beam width.

CHAPTER THREE

3 MATERIALS AND METHODS

3.1 Overview

This chapter presents the materials and procedures that were used for the study. It involves the description of the CT facility, the procedure employed with the use of a 100-mm Ion Chamber with integrated electrometer and procedure employed with the use of the Barracuda electrometer in the estimation of CTDI values.

3.2 Materials

The materials that were used for this research work included;

1. 16 slice Siemens CT scanner (Siemens Somatom Emotion, Forchheim, Germany)
2. Standard CT dosimetry PMMA cylindrical acrylic head and body phantoms (PTW, Freighburg, Germany)
3. 100-mm pencil Ion Chamber with integrated electrometer (PTW Freighburg, Germany)
4. CT Dose Profiler Probe (RTI Electronics, Sweden)
5. Barracuda with Ocean Software interface (RTI Electronics, Sweden)
6. Microsoft Excel spreadsheet (2016)

3.2.1 The CT Scanner

In this research work, the dose estimation was performed on a Siemens Somatom Emotion CT multi detector scanner (Siemens Healthcare, Forchheim, Germany). The scanner has a 16 channel detector configuration with a small focal spot capable of making a 16 × 1.2mm multi-slice imaging. It was

installed at Sweden Ghana Medical Centre in 2011. The scanner has tube potentials of 80kVp, 110kVp and 130kVp. A specific voltage is selected depending on what application and protocols employed. The scanner has automatic exposure feature (CareDose4D) and can also be operated manually as with this study. In cases where the CareDose4D is employed, the tube current is automatically adjusted whilst the operator selects the specified parameters including tube voltage and current if operated manually. For this study, a tube potential of 130kVp, slice thickness of 4mm and 5mm with tube current-time products from 80 – 300 mAs were used in both techniques for the examination protocols. Plate 3.1 shows the Siemens CT employed in this work.

Plate 3.1: Siemens CT Scanner used for the study [Field work, 2016]

3.2.2 The PMMA CT Phantoms

Two different cylindrical CT dosimetry phantoms; 16-cm diameter CT head phantom and 32-cm diameter CT body phantom made from acrylic polymethyl methacrylate (PMMA) were used for the CTDI estimations from the Siemens Somatom CT scanner.

The 16-cm diameter CT head phantom mimics the adult head as well as the pediatric body in some cases for CT examinations and the 32-cm diameter CT body phantom mimics the adult body for CT examinations. They both have five 1-cm holes within them for the insertion of CT dose profiler and Ion Chamber. The holes are located at the center and 1-cm depth at the peripheral of the phantom, specifically at 12 –, 3 –, 6 – and 9 – O'clock positions. Plate 3.2 below shows images of the CT head and body phantoms.

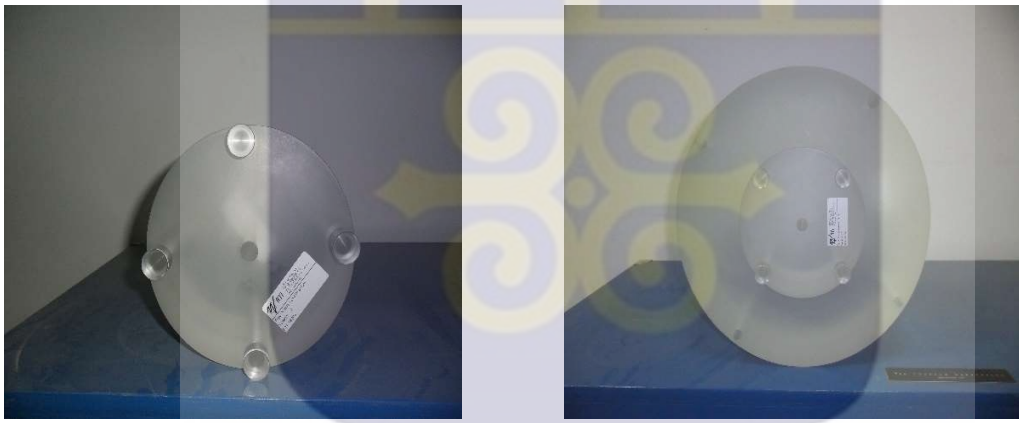

Plate 3.2: Image of CT head phantom (left) and body phantom (right) [Field work, 2016]

3.2.3 The PTW Ion Chamber and Electrometer

The Ion Chamber represents a pencil type chamber that is used for measurements within a CT body or head phantom or sometimes in air. It is intended to be used with an electrometer for the determination of Dose Length Product (DLP) and CTDI values. The pencil Ion Chamber is 100mm in length, sensitive along the entire length and shows a homogeneous response over the whole length. The Ion Chamber is a CT chamber type 30009, manufactured by PTW in Freiburg, Germany, is a

vented cylinder chamber that is made for the measurements of photon radiation in computed tomography. The electrometer records charges or Dose Length Products in the units of coulombs or mGy.cm respectively when used with the Ion Chamber. Figure 3.1 below shows an image of a CT Ion Chamber and an electrometer.

Figure 3.1: Image of CT Ion Chamber (left) and electrometer (right) [PTW chamber type 30009, Freiburg, Germany]

3.2.4 The CT Dose Profiler Probe

The CT Dose Profiler probe is a detector that is used to estimate point dose with a solid-state sensor (3cm from the end of the probe). It has a thin diode of thickness 300 µm and size 2x2 mm and it is more sensitive than the CT pencil Ion Chamber. There is aluminium filled Plexiglas that house the probe. The probe has the tendency to be extended by a 45mm length PMMA extension piece to fit into different phantoms. The solid-state sensor is very thin and small (250 µm) and that makes it completely irradiated in the beam. When the sensor is irradiated at a time, the detector registers the

dose value at that point and sends the data to the Barracuda. It was manufactured by RTI Electronics in Sweden. Figure 3.2 below shows an image of CT Dose Profiler Probe

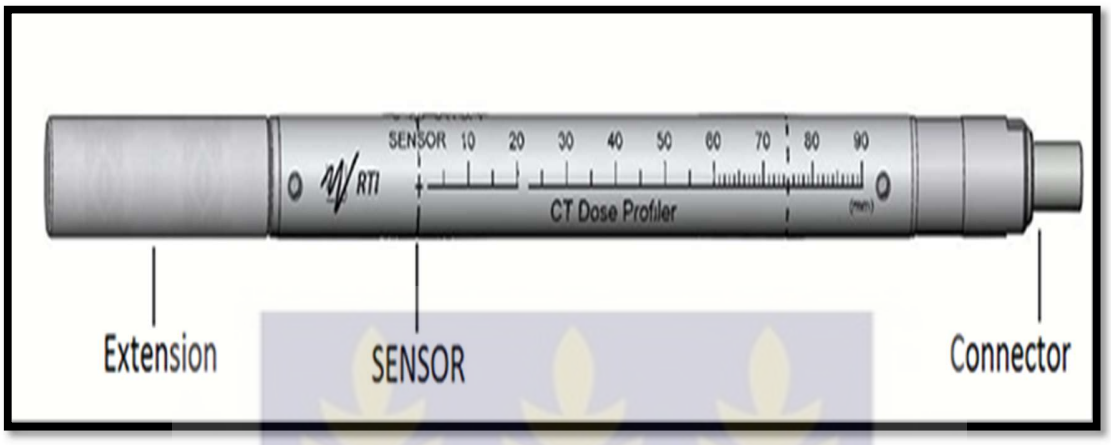

Figure 3.2: Diagram of CT Dose Profiler Probe (www.rti.se, RTI Electronics, Sweden)

3.2.5 The Barracuda

The Barracuda is a solid state detector which is housed in a metal for durability purpose. It can be used in mammography, fluoroscopy, dental radiography, Computed Tomography and other modalities. It has auto compensation to ensure that data is accurate without any manual corrections to measured kVp and dose readings. It is connected to the CT Dose Profiler (CTDP) probe at one side and to the PC with an Ocean software interface at the other end for CTDI estimations.

Figure 3.3: Diagram of a Barracuda (www.rti.se, RTI Electronics, Sweden)

3.3 Experimental Method

3.3.1 Measurement of Dose

Radiation doses were measured with the Dose Profiler probe which is connected to the Barracuda and with the PTW Ion Chamber which is also connected to the electrometer (PTW Diados E). The measurements of dose were done for CT head and routine body (chest, abdomen and pelvis) phantoms during the study. The study begun by setting up the CT head phantom on the CT couch. The head phantom was positioned at the isocenter of the CT scanner and the long axis of the head phantom was aligned with the z-axis of the scanner.

3.3.2 Dose Measurement with the PTW Ion Chamber

The PTW pencil Ion Chamber which is connected to an electrometer with a cable was placed in the central hole of the head phantom. Two horizontal lasers in the CT room were adjusted to be visible on the mid-line of the Ion Chamber and a vertical laser was also set to be visible at the middle of the phantom. This was done to properly align the phantom and the chamber on the couch.

The cable connecting the Ion Chamber and the electrometer was tapped on the couch to prevent dislodging of the Ion Chamber from the phantom. The CT room was locked for radiation protection reasons. A topogram of the head phantom was taken and the required volume was selected. Parameters such as tube potential, tube current and slice thickness were selected whiles other parameters were kept constant for the examination. A tube potential of 130kVp, tube current-time product of 240mA, pitch of 0.55 and slice thickness of 4mm were selected for the first scan. Measurements were taken at the periphery sites of 12 –, 3 –, 6 – and 9 – O'clock as well which can also be represented as P1, P2, P3 and P4 respectively. The procedure was repeated with different values of tube current-time product but with all other parameters constant. Tube currents of 220mA, 240mA, 260mA and 280mA were used in the procedure for the CT head phantom scan. Different

values were chosen to provide range of data that can be analyzed to check the validity of the dose measuring techniques. Parameters used for the examination can be found in Table 3.1 below.

Table 3.1: Scan Parameters used for the CT examination

Examination	KVp	mAs	Slice Thickness (mm)	Pitch
Head	130	120	4	0.55
Body	130	80	5	0.8
Head	130	140	4	0.55
Body	130	100	5	0.8
Head	130	160	4	0.5
Body	130	120	5	0.8
Head	130	180	4	0.55
Body	130	140	5	0.8
Head	130	200	4	0.55
Body	130	160	5	0.8
Head	130	220	4	0.55
Body	130	180	5	0.8
Head	130	240	4	0.55
Body	130	200	5	0.8
Head	130	260	4	0.55
Body	130	210	5	0.8
Head	130	280	4	0.55
Body	130	220	5	0.8
Head	130	300	4	0.55

After the head phantom measurements were done, the procedure was repeated for the CT body phantom. Charges were measured and recorded in each scan. The charges measured and recorded from the electrometer were used to estimate CTDI values in the study with the use of integral and other mathematical equations. Table 3.2 shows mathematical expressions and descriptions for MSAD and CTDI measurements.

Table 3.2: Mathematical expressions and descriptions for MSAD and CTDI variations

Dose Index	**Mathematical Expression**	**Description**
Multiple Scan average dose	$MSAD = \frac{1}{I}\int_{-I/2}^{+I/2} D_{N,I}(z)dz$	Measured with multiple TLDs and scans; represents the average dose over one scan interval (I) in the central portion of a multiple scan (N) dose profile with a negligible dose contribution from the first and last scans
CT dose index	$CTDI_{\infty} = \frac{1}{T}\int_{-\infty}^{+\infty} D(z)dz$	It is equal to MSAD if all the scatter tails are included and the nominal section thickness equals the scan interval ($T = I$); measured with one scan by using one Ion Chamber or multiple TLDs
CTDI as defined by the FDA	$CTDI_{FDA} = \frac{1}{NT}\int_{-7T}^{+7T} D(z)dz$	TLDs used to measure in order to obtain correct integration limits
CTDI measured over 100mm chamber	$CTDI_{100} = \frac{1}{NT}\int_{-50mm}^{+50mm} D(z)dz$	Measured with a 100mm pencil Ion Chamber
Weighted CTDI	$CTDI_w = \frac{1}{3}CTDI_{100,center} + \frac{2}{3}CTDI_{100,periphery}$	Uses mean $CTDI_{100}$ measurements
Volume CTDI	$CTDI_{vol} = \frac{NT}{I}CTDI_w = \frac{CTDI_w}{pitch}$	Uses $CTDI_w$ measurements

FDA – U. S. Food and Drug Administration

The electrometer readings were taken in charge mode and corrected for temperature and pressure. Equation (1) was needed for temperature and pressure correction, but the temperature of 25 degree-celcius and 100.56 mmHg recorded in the experimental room was within a range specified by the Ion Chamber manufacturer where there was no need for temperature and pressure correction. The charges recorded from the electrometer are shown in Appendices B and C respectively.

$$P_{TP} = \frac{273 \quad .2 \; + \; T}{273 \quad .2 \; + \; 22} * \frac{101 \quad .33}{P} \tag{9}$$

Where,

T – Temperature measured in the study room

P – Pressure in the room

P_{TP} – correction for pressure and temperature

The charges were converted into Exposure (rad) using equation (2). $CTDI_{100}$, $CTDI_w$ and $CTDI_{vol}$ were then estimated using equations (3), (4) and (5) respectively from AAPM Report 96.

$$X(rad) = \frac{Q}{m_{air}}(C/kg) = \frac{Q}{m_{air}} \cdot \frac{1}{2.58 \times 10^{-4}}(R) \cdot f_{med}(rad/R) \tag{10}$$

$$CTDI_{100} = \frac{X(rad) \cdot C_f \cdot L(mm)}{N \cdot T(mm)} \tag{11}$$

$$CTDI_w = \frac{1}{3} CTDI_{100}^{centre} + \frac{2}{3} CTDI_{100}^{periphery} \tag{12}$$

$$CTDI_{vol} = \frac{CTDI_w}{p_f} \tag{13}$$

where,

Q represents charges recorded in coulombs

f_{med} represents [Exposure to dose conversion factor] = 0.78 rad/R,

C_f represents [Electrometer/Ion Chamber calibration factor] = 1,

L represents [Ion Chamber length] = 100 mm,

T = Width of one slice or tomographic selection,

N represents [Number of slices or tomographic sections imaged in a single axial scan] = 16,

X represents [Estimated exposure] = Q/m

P_f = Pitch factor used

m_{air} represents [Mass of air irradiated] = $\rho_{air} \times v_{air}$

ρ_{air} represents [Density of air at Standard Temperature and Pressure] = 1.293 kg/m3

v_{air} represents [Vol. of irradiated air for single slice] = (slice thickness/100 mm) × v_c

v_c represents [Vol. of Ion Chamber] = 3.14 cm^3 = 3.14 × 10^{-6} m^3

Plate 3.3 below shows the set-up of the measurement with the Ion Chamber.

Plate 3.3: Experimental set-up for the measurement of CTDI with the Ion Chamber [Field work, 2016]

3.3.3 Dose Measurements with the RTI Dose Profiler Probe and Barracuda

A CT Dose Profiler Probe was connected to a Barracuda with an extension cable and the Barracuda was subsequently connected to a computer which had the Ocean Software interface. The Dose Profiler probe was placed in the middle hole of the CT head phantom. The horizontal and vertical lasers were used for proper alignment just like in the set-up with the Ion Chamber. The cable was tapped to prevent dislodging of the probe from the phantom in this set up too.

The same procedure and parameters as used for the dose measurements with the Ion Chamber were used for the dose measurements with the dose profiler. After taken measurements for the head phantom, the procedure was repeated for body phantom measurements as well. The Dose-Length Products, Computed Tomography Dose Index weighted ($CTDI_w$) and volume Computed Tomography Dose Index ($CTDI_{vol}$) were automatically generated by the Barracuda in each scan. Plate 3.4 below shows the experimental set-up of the dose measurements with the dose profiler probe.

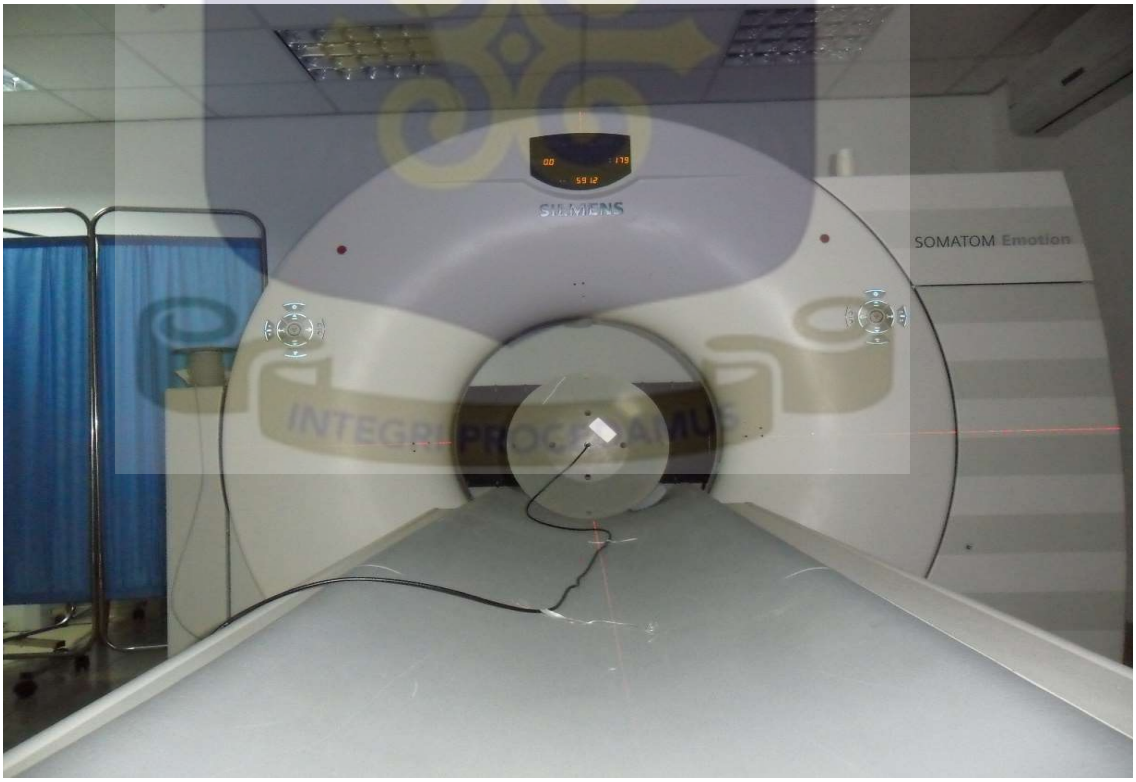

Plate 3.4: Experimental set-up for the measurement of CTDI with the dose profiler probe [Field work, 2016]

CHAPTER FOUR

4 RESULTS AND DISCUSSION

4.1 Overview

This chapter presents the results obtained from the CT dose measurements made on the CT head and body phantoms with the use of Ion Chamber technique and that obtained using the Barracuda technique for the validation of CTDI values from the latter technique. The results are further analyzed and discussed in this section.

4.2 Results

4.2.1 Measurements of CTDI with the Ion Chamber Technique

Tables 4.1 – 4.9 show the charges recorded during the acrylic CT head PMMA phantom examination with the use of the Ion Chamber in the study and the subsequent calculated exposure, $CTDI_w$ and $CTDI_{vol}$ values using mathematical expressions. Average Charge, Exposure, $CTDI_{100}$, weighted Computed Tomography Dose Index ($CTDI_w$) and volume Computed Tomography Dose Index ($CTDI_{vol}$) are represented in the Tables.

Table 4.1 CTDI values for head phantom at 130kVp and 140mAs

	Charge	Exposure		
	Q_{avg} (nC)	X (C/kg)	X (rad)	$CTDI_{100}$
Central (C)	0.1314	0.000809	2.4464	1.5290
Periphery (P_1)	0.1615	0.000994	3.0064	1.8790
Periphery (P_2)	0.1628	0.001002	3.0302	1.8939
Periphery (P_3)	0.1638	0.001009	3.0501	1.9063
Periphery (P_4)	0.1634	0.001006	3.0421	1.9013
	$CTDI_{100c}$ (rad)	$CTDI_{100p}$ (rad)	$CTDI_w$ (mGy)	$CTDI_{vol}$ (mGy)
	1.5290	1.8951	17.7308	32.2378

Table 4.2: CTDI values for head phantom at 130kVp and 160mAs

	Charge	Exposure		
	Q_{avg} (nC)	X (C/kg)	X (rad)	$CTDI_{100}$
Central (C)	0.1320	0.000813	2.4573	1.5358
Periphery (P_1)	0.1622	0.000999	3.0198	1.8874
Periphery (P_2)	0.1635	0.001007	3.0437	1.9023
Periphery (P_3)	0.1646	0.001013	3.0637	1.9148
Periphery (P_4)	0.1641	0.001011	3.0557	1.9098
	$CTDI_{100c}$ (rad)	$CTDI_{100p}$ (rad)	$CTDI_w$ (mGy)	$CTDI_{vol}$ (mGy)
	1.5358	1.9036	17.8100	32.3818

Table 4.3: CTDI values for head phantom at 130kVp and 180mAs

	Charge	Exposure		
	Q_{avg} (nC)	X (C/kg)	X (rad)	$CTDI_{100}$
Central (C)	0.1478	0.000910	2.7522	1.7201
Periphery (P_1)	0.1817	0.001119	3.3822	2.1139
Periphery (P_2)	0.1831	0.001128	3.4090	2.1306
Periphery (P_3)	0.1843	0.001135	3.4313	2.1446
Periphery (P_4)	0.1838	0.001132	3.4224	2.1390
	$CTDI_{100c}$ (rad)	$CTDI_{100p}$ (rad)	$CTDI_w$ (mGy)	$CTDI_{vol}$ (mGy)
	1.7201	2.1320	19.9472	36.2676

Table 4.4: CTDI values for head phantom at 130kVp and 200mAs

	Charge	Exposure		
	Q_{avg} (nC)	X (C/kg)	X (rad)	$CTDI_{100}$
Central (C)	0.1541	0.000949	2.8687	1.7930
Periphery (P_1)	0.1935	0.001192	3.6022	2.2514
Periphery (P_2)	0.1946	0.001198	3.6218	2.2636
Periphery (P_3)	0.1956	0.001204	3.6413	2.2758
Periphery (P_4)	0.1952	0.001202	3.6339	2.2712
	$CTDI_{100c}$ (rad)	$CTDI_{100p}$ (rad)	$CTDI_w$ (mGy)	$CTDI_{vol}$ (mGy)
	1.7930	2.2655	21.0798	38.3270

Table 4.5: CTDI values for head phantom at 130kVp and 220mAs

	Charge	Exposure		
	Q_{avg} (nC)	X (C/kg)	X (rad)	$CTDI_{100}$
Central (C)	0.1643	0.001011	3.0580	1.9113
Periphery (P_1)	0.2019	0.001243	3.7580	2.3487
Periphery (P_2)	0.2035	0.001253	3.7878	2.3673
Periphery (P_3)	0.2048	0.001261	3.8126	2.3829
Periphery (P_4)	0.2043	0.001258	3.8027	2.3767
	$CTDI_{100c}$ (rad)	$CTDI_{100p}$ (rad)	$CTDI_w$ (mGy)	$CTDI_{vol}$ (mGy)
	1.9113	2.3689	22.1635	40.2973

Table 4.6: CTDI values for head phantom at 130kVp and 240mAs

	Charge	Exposure		
	Q_{avg} (nC)	X (C/kg)	X (rad)	$CTDI_{100}$
Central (C)	0.1807	0.001113	3.3638	2.1024
Periphery (P_1)	0.2221	0.001367	4.1338	2.5836
Periphery (P_2)	0.2238	0.001378	4.1665	2.6041
Periphery (P_3)	0.2253	0.001387	4.1938	2.6211
Periphery (P_4)	0.2247	0.001384	4.1829	2.6143
	$CTDI_{100c}$ (rad)	$CTDI_{100p}$ (rad)	$CTDI_w$ (mGy)	$CTDI_{vol}$ (mGy)
	2.1024	2.6058	24.3799	44.3270

Table 4.7: CTDI values for head phantom at 130kVp and 260mAs

	Charge	Exposure		
	Q_{avg} (nC)	X (C/kg)	X (rad)	$CTDI_{100}$
Central (C)	0.1971	0.001214	3.6696	2.2935
Periphery (P_1)	0.2422	0.001492	4.5096	2.8185
Periphery (P_2)	0.2442	0.001503	4.5453	2.8408
Periphery (P_3)	0.2458	0.001513	4.5751	2.8594
Periphery (P_4)	0.2451	0.001509	4.5632	2.8520
	$CTDI_{100c}$ (rad)	$CTDI_{100p}$ (rad)	$CTDI_w$ (mGy)	$CTDI_{vol}$ (mGy)
	2.2935	2.8427	26.5962	48.3568

Table 4.8: CTDI values for head phantom at 130kVp and 280mAs

	Charge	Exposure		
	Q_{avg} (nC)	X (C/kg)	X (rad)	$CTDI_{100}$
Central (C)	0.2135	0.001315	3.9754	2.4846
Periphery (P_1)	0.2624	0.001616	4.8854	3.0534
Periphery (P_2)	0.2645	0.001629	4.9241	3.0776
Periphery (P_3)	0.26624	0.001639	4.9564	3.0977
Periphery (P_4)	0.2655	0.001635	4.9434	3.0897
	$CTDI_{100c}$ (rad)	$CTDI_{100p}$ (rad)	$CTDI_w$ (mGy)	$CTDI_{vol}$ (mGy)
	2.4846	3.0796	28.8126	52.3865

Table 4.9: CTDI values for head phantom at 130kVp and 300mAs

	Charge	Exposure		
	Q_{avg} (nC)	X (C/kg)	X (rad)	$CTDI_{100}$
Central (C)	0.2300	0.001416	4.2812	2.6758
Periphery (P_1)	0.2826	0.001740	5.2612	3.2882
Periphery (P_2)	0.2849	0.001754	5.3029	3.3143
Periphery (P_3)	0.28672	0.001766	5.3376	3.3360
Periphery (P_4)	0.2860	0.001761	5.3237	3.3273
	$CTDI_{100c}$ (rad)	$CTDI_{100p}$ (rad)	$CTDI_w$ (mGy)	$CTDI_{vol}$ (mGy)
	2.6758	3.3165	31.0289	56.4162

Table 4.10 – Table 4.18 show results for the CT body phantom dose measurement with the use of the Ion Chamber technique

Table 4.10: CTDI values for body phantom at 130kVp and 80mAs (Abdomen scan)

	Charge	Exposure		
	Q_{avg} (nC)	X (C/kg)	X (rad)	$CTDI_{100}$
Central (C)	0.0668	0.000411	1.2426	0.6213
Periphery (P_1)	0.0883	0.000543	1.6429	0.8214
Periphery (P_2)	0.0885	0.000545	1.6475	0.8238
Periphery (P_3)	0.0875	0.000539	1.6289	0.8145
Periphery (P_4)	0.0880	0.000542	1.6382	0.8191
	$CTDI_{100c}$ (rad)	$CTDI_{100p}$ (rad)	$CTDI_w$ (mGy)	$CTDI_{vol}$ (mGy)
	0.6213	0.8197	7.5356	9.4196

Table 4.11: CTDI values for head phantom at 130kVp and 100mAs (Abdomen scan)

	Charge	Exposure		
	Q_{avg} (nC)	X (C/kg)	X (rad)	$CTDI_{100}$
Central (C)	0.0899	0.000554	1.6736	0.8368
Periphery (P_1)	0.0939	0.000578	1.7481	0.8740
Periphery (P_2)	0.0942	0.000580	1.7536	0.8768
Periphery (P_3)	0.0945	0.000582	1.7592	0.8796
Periphery (P_4)	0.0938	0.000578	1.7462	0.8731
	$CTDI_{100c}$ (rad)	$CTDI_{100p}$ (rad)	$CTDI_w$ (mGy)	$CTDI_{vol}$ (mGy)
	0.8368	0.8759	8.6286	10.7857

Table 4.12: CTDI values for head phantom at 130kVp and 120mAs (Abdomen scan)

	Charge	Exposure		
	Q_{avg} (nC)	X (C/kg)	X (rad)	$CTDI_{100}$
Central (C)	0.1079	0.000664	2.0083	1.0042
Periphery (P_1)	0.1127	0.000694	2.0977	1.0488
Periphery (P_2)	0.1130	0.000696	2.1044	1.0522
Periphery (P_3)	0.1134	0.000698	2.1111	1.0555
Periphery (P_4)	0.1126	0.000693	2.0954	1.0477
	$CTDI_{100c}$ (rad)	$CTDI_{100p}$ (rad)	$CTDI_w$ (mGy)	$CTDI_{vol}$ (mGy)
	1.0042	1.0511	10.3543	12.9429

Table 4.13: CTDI values for head phantom at 130kVp and 140mAs (Abdomen scan)

	Charge	Exposure		
	Q_{avg} (nC)	X (C/kg)	X (rad)	$CTDI_{100}$
Central (C)	0.1271	0.000783	2.3661	1.1831
Periphery (P_1)	0.1328	0.000817	2.4713	1.2356
Periphery (P_2)	0.1329	0.000818	2.4741	1.2370
Periphery (P_3)	0.1329	0.000818	2.4741	1.2370
Periphery (P_4)	0.1331	0.000819	2.4769	1.2384
	$CTDI_{100c}$ (rad)	$CTDI_{100p}$ (rad)	$CTDI_w$ (mGy)	$CTDI_{vol}$ (mGy)
	1.1831	1.2370	12.1905	15.2381

Table 4.14: CTDI values for head phantom at 130kVp and 160mAs (Chest scan)

	Charge	Exposure		
	Q_{avg} (nC)	X (C/kg)	X (rad)	$CTDI_{100}$
Central (C)	0.1500	0.000924	2.7924	1.3962
Periphery (P_1)	0.1861	0.001146	3.4645	1.7322
Periphery (P_2)	0.1861	0.001146	3.4635	1.7318
Periphery (P_3)	0.1862	0.001147	3.4663	1.7332
Periphery (P_4)	0.1861	0.001146	3.4635	1.7318
	$CTDI_{100c}$ (rad)	$CTDI_{100p}$ (rad)	$CTDI_w$ (mGy)	$CTDI_{vol}$ (mGy)
	1.3962	1.7322	16.2022	20.2528

Table 4.15: CTDI values for head phantom at 130kVp and 180mAs (Chest scan)

	Charge	Exposure		
	Q_{avg} (nC)	X (C/kg)	X (rad)	$CTDI_{100}$
Central (C)	0.1688	0.001039	3.1415	1.5707
Periphery (P_1)	0.2094	0.001289	3.8975	1.9488
Periphery (P_2)	0.2093	0.001289	3.8965	1.9482
Periphery (P_3)	0.2095	0.001290	3.8996	1.9498
Periphery (P_4)	0.2093	0.001289	3.8965	1.9482
	$CTDI_{100c}$ (rad)	$CTDI_{100p}$ (rad)	$CTDI_w$ (mGy)	$CTDI_{vol}$ (mGy)
	1.5707	1.9488	18.2275	22.7844

Table 4.16: CTDI values for head phantom at 130kVp and 200mAs (Chest scan)

	Charge	Exposure		
	Q_{avg} (nC)	X (C/kg)	X (rad)	$CTDI_{100}$
Central (C)	0.1875	0.001155	3.4905	1.7453
Periphery (P_1)	0.2326	0.001432	4.3306	2.1653
Periphery (P_2)	0.2326	0.001432	4.3294	2.1647
Periphery (P_3)	0.2328	0.001433	4.3329	2.1664
Periphery (P_4)	0.2326	0.001432	4.3294	2.1647
	$CTDI_{100c}$ (rad)	$CTDI_{100p}$ (rad)	$CTDI_w$ (mGy)	$CTDI_{vol}$ (mGy)
	1.7453	2.1653	20.2528	25.3160

Table 4.17: CTDI values for head phantom at 130kVp and 210mAs (Pelvis scan)

	Charge	Exposure		
	Q_{avg} (nC)	X (C/kg)	X (rad)	$CTDI_{100}$
Central (C)	0.2410	0.001484	4.4865	2.2432
Periphery (P_1)	0.3151	0.001940	5.8659	2.9330
Periphery (P_2)	0.3151	0.001940	5.8659	2.9330
Periphery (P_3)	0.3148	0.001938	5.8604	2.9302
Periphery (P_4)	0.3153	0.001942	5.8697	2.9348
	$CTDI_{100c}$ (rad)	$CTDI_{100p}$ (rad)	$CTDI_w$ (mGy)	$CTDI_{vol}$ (mGy)
	2.2432	2.9327	27.0290	33.7863

Table 4.18: CTDI values for head phantom at 130kVp and 220mAs (Pelvis scan)

	Charge	Exposure		
	Q_{avg} (nC)	X (C/kg)	X (rad)	$CTDI_{100}$
Central (C)	0.2560	0.001576	4.7657	2.3829
Periphery (P_1)	0.3300	0.002032	6.1433	3.0717
Periphery (P_2)	0.3311	0.002038	6.1629	3.0814
Periphery (P_3)	0.3311	0.002039	6.1638	3.0819
Periphery (P_4)	0.3315	0.002041	6.1712	3.0856
	$CTDI_{100c}$ (rad)	$CTDI_{100p}$ (rad)	$CTDI_w$ (mGy)	$CTDI_{vol}$ (mGy)
	2.3829	3.0802	28.4772	35.5965

4.2.2 Measurements of CTDI with the CT Dose Profiler Probe and Barracuda Technique

The CTDI values obtained from the Barracuda technique for the radiation dose measurement for the CT head and body phantoms can be found in Tables 4.19 and 4.20 respectively.

Table 4.19: CTDI values for head phantom at 130kVp and varying mAs

kVp	mAs	$CTDI_w$ (mGy)	$CTDI_{vol}$ (mGy)
130	140	17.60	32.9
130	160	18.50	33.4
130	180	18.95	34.5
130	200	20.44	37.2
130	220	22.53	41.0
130	240	24.55	44.6
130	260	26.40	50.7
130	280	27.86	51.4
130	300	29.12	53.0

Table 4.20: CTDI values for body phantom at 130kVp and varying mAs

kVp	mAs	Examination	$CTDI_w$ (mGy)	$CTDI_{vol}$ (mGy)
130	80	Abdomen	8	9.5
130	100	Abdomen	9	11.2
130	120	Abdomen	11	13.5
130	140	Abdomen	13	15.6
130	160	Chest	17	19.0
130	180	Chest	19	21.4
130	200	Chest	21	23.8
130	210	Pelvis	25	37.0
130	220	Pelvis	26	39.0

4.2.3 Representation of the CTDI values from the Measurement Techniques

The $CTDI_w$ and $CTDI_{vol}$ values obtained from both techniques are presented in Figures 4.1 – 4.4 for the head and body phantoms examinations.

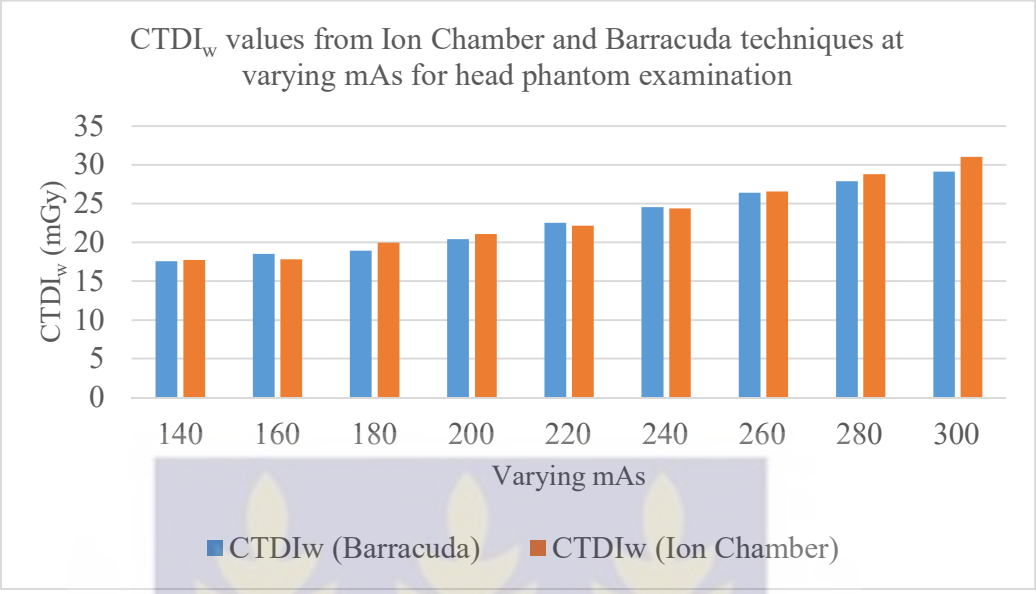

Figure 4.1: Graphical representation of $CTDI_w$ values for head phantom examination

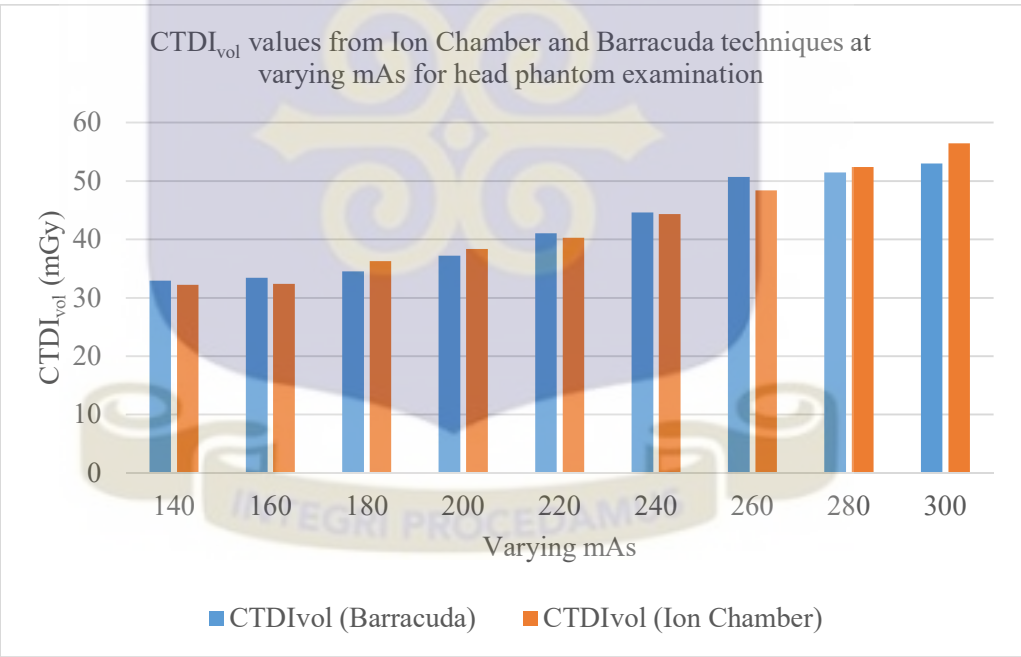

Figure 4.2: Graphical representation of $CTDI_{vol}$ values for the head phantom examination

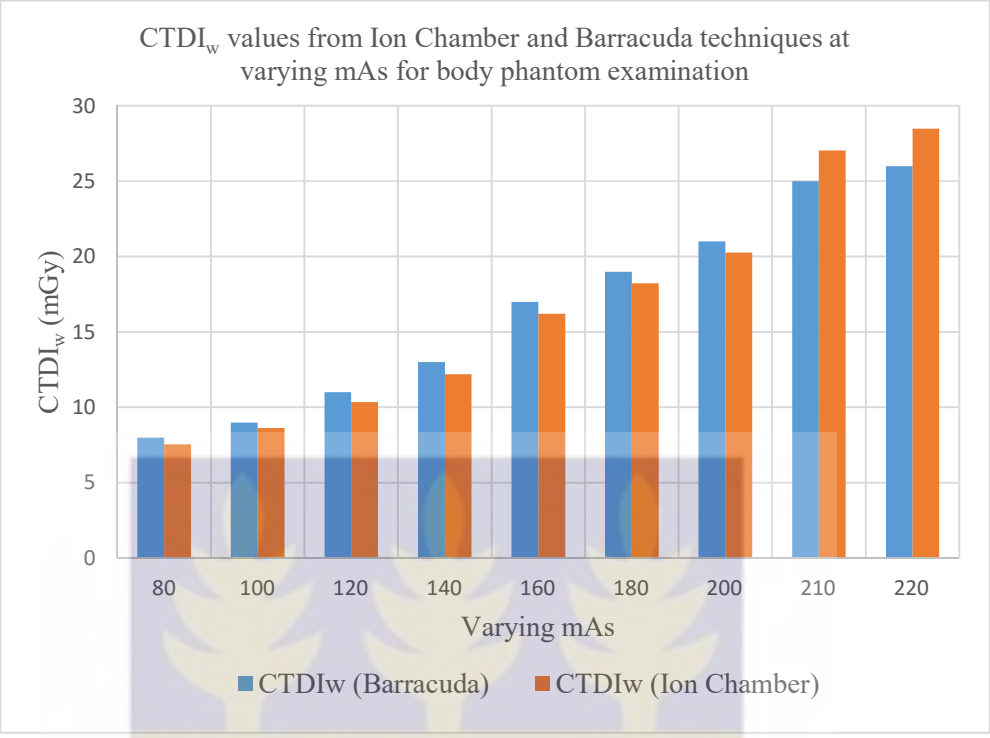

Figure 4.3: Graphical representation of CTDIw values for the body phantom examination

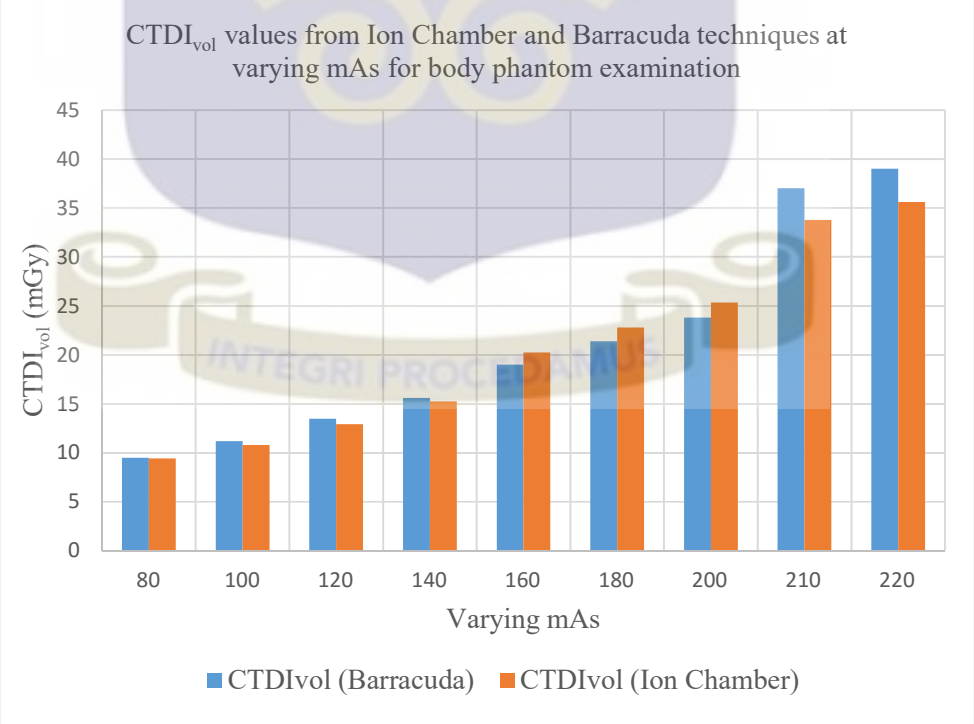

Figure 4.4: Graphical representation of $CTDI_{vol}$ values for the body phantom examination

4.2.4 Deviations of CTDI values

Tables 4.21 and 4.22 presents the percentage deviations of the CTDI values measured from the Ion Chamber technique to that measured from the Barracuda technique for the head and body phantom examinations respectively.

Table 4.21: Deviation of CTDI values for head phantom at 130kVp and varying mAs

Varying mAs	Barracuda $CTDI_w$ (mGy)	Ion Chamber $CTDI_w$ (mGy)	Barracuda $CTDI_{vol}$ (mGy)	Ion Chamber $CTDI_{vol}$ (mGy)	% Deviation ($CTDI_w$)	% Deviation ($CTDI_{vol}$)
140	17.60	17.73	32.90	32.24	4.16	3.50
160	18.5	17.81	33.40	32.38	-1.19	1.58
180	18.95	19.95	34.50	36.27	-5.26	-5.12
200	20.44	21.08	37.20	38.33	-3.13	-3.03
220	22.53	22.16	41.00	40.30	1.63	1.71
240	24.55	24.38	44.60	44.33	0.69	0.61
260	26.4	26.60	50.70	48.36	-0.74	4.62
280	27.86	28.81	51.40	52.39	-3.42	-1.92
300	29.12	31.03	53.00	56.42	-6.56	-6.45
StDev.	4.3	4.8	8.1	8.6		

Table 4.22: Deviation of CTDI values for body phantom at 130kVp and varying mAs

Varying mAs	Barracuda $CTDI_w$ (mGy)	Ion Chamber $CTDI_w$ (mGy)	Barracuda $CTDI_{vol}$ (mGy)	Ion Chamber $CTDI_{vol}$ (mGy)	% Deviation ($CTDI_w$)	% Deviation ($CTDI_{vol}$)
80	8.00	7.54	9.50	9.42	5.80	0.85
100	9.00	8.63	11.20	10.79	4.13	3.70
120	11.00	10.35	13.50	12.94	5.87	4.13
140	13.00	12.19	15.60	15.24	6.23	2.32
160	17.00	16.20	19.00	20.25	4.70	-6.59
180	19.00	18.23	21.40	22.78	4.07	-6.47
200	21.00	20.25	23.80	25.32	3.56	-6.37
210	25.00	27.03	37.00	33.79	-8.12	8.69
220	26.00	28.48	39.00	35.60	-9.53	8.73
StDev	6.7	7.7	10.6	9.6		

Table 4.23: Comparison of Measured and Console Displayed CTDI values for head phantom examinations at 130kVp

Varying mAs	Console Displayed $CTDI_w$ (mGy)	Console Displayed $CTDI_{vol}$ (mGy)	Barracuda $CTDI_w$ (mGy)	Ion Chamber $CTDI_w$ (mGy)	Barracuda $CTDI_{vol}$ (mGy)	Ion Chamber $CTDI_{vol}$ (mGy)	% $CTDI_w$ Deviation (CD and Barracuda)	% $CTDI_w$ Deviation (CD and Ion Chamber)	% $CTDI_{vol}$ Deviation (CD and Barracuda)	% $CTDI_{vol}$ Deviation (CD and Ion Chamber)
140	19.19	31.01	17.60	17.73	32.90	32.24	9.03	8.23	-5.74	-3.82
160	20.32	33.84	18.5	17.81	33.40	32.38	9.84	14.01	1.31	4.50
180	22.00	36.76	18.95	19.95	34.50	36.27	16.01	10.28	6.55	1.35
200	23.12	39.25	20.44	21.08	37.20	38.33	13.11	9.68	5.51	2.40
220	24.25	42.31	22.53	22.16	41.00	40.30	7.63	9.43	3.20	4.99
240	25.10	45.00	24.55	24.38	44.60	44.33	2.24	2.95	0.90	1.51
260	27.90	49.21	26.4	26.60	50.70	48.36	5.68	4.89	-2.94	1.76
280	29.35	53.41	27.86	28.81	51.40	52.39	5.35	1.87	3.91	1.95
300	32.21	58.24	29.12	31.03	53.00	56.42	10.61	3.8	9.89	3.23
StDev.	4.3	9.10	4.3	4.8	8.1	8.6				

Table 4.24: Comparison of Measured and Console Displayed CTDI values for body phantom examinations at 130kVp

Varying mAs	Console Displayed $CTDI_w$ (mGy)	Console Displayed $CTDI_{vol}$ (mGy)	Barracuda $CTDI_w$ (mGy)	Ion Chamber $CTDI_w$ (mGy)	Barracuda $CTDI_{vol}$ (mGy)	Ion Chamber $CTDI_{vol}$ (mGy)	% $CTDI_w$ Deviation (CD and Barracuda)	% $CTDI_w$ Deviation (CD and Ion Chamber)	% $CTDI_{vol}$ Deviation (CD and Barracuda)	% $CTDI_{vol}$ Deviation (CD and Ion Chamber)
80	8.21	9.20	8.00	7.54	9.50	9.42	2.63	8.89	-3.16	-2.34
100	9.02	11.85	9.00	8.63	11.20	10.79	0.22	4.52	5.80	9.82
120	11.99	13.93	11.00	10.35	13.50	12.94	9.00	15.85	3.19	7.65
140	14.11	16.54	13.00	12.19	15.60	15.24	8.54	15.75	6.03	8.53
160	17.52	19.99	17.00	16.20	19.00	20.25	3.06	8.19	5.21	-1.28
180	20.12	24.00	19.00	18.23	21.40	22.78	5.89	10.37	12.15	5.36
200	23.09	26.52	21.00	20.25	23.80	25.32	9.95	14.02	11.43	4.74
210	26.85	35.21	25.00	27.03	37.00	33.79	7.4	-0.67	-4.84	4.20
220	28.08	38.09	26.00	28.48	39.00	35.60	8	-1.40	-2.33	7.00
StDev.	7.4	10.1	6.7	7.7	10.6	9.6				

4.3 Discussions

In analyzing the results for the CT head phantom examination, the minimum $CTDI_{vol}$ deviation recorded between the two measurement devices and techniques was 0.61% when the scan protocol was set at fixed exposure parameter of 130kVp and tube current-time product of 240mAs. The maximum $CTDI_{vol}$ deviation was also measured at -6.45% when the scan protocol for the CT head examination was set at a fixed exposure parameter and tube current-time product of 130kVp and 300mAs respectively. When the tube current-time products were varied between 140mAs to 300mAs, there were mean $CTDI_{vol}$ of (42.3 $\pm$ 8.6) mGy and (42.1 $\pm$ 8.1) mGy for Barracuda and Ion Chamber techniques respectively with a mean deviation of 1.4 mGy between them.

In reference to the $CTDI_w$ for the CT head examination, there was a minimum $CTDI_w$ deviation of 0.69% at exposure parameter of 130kVp and tube current-time product of 240mAs between the two techniques. The maximum $CTDI_w$ deviation was also estimated at -6.56% between the techniques with scan protocol of 130kVp and 300mAs. With a fixed tube potential of 130kVp and varying tube current-time products from 140mAs to 300mAs, there were average $CTDI_w$ of (22.9 $\pm$ 4.3) mGy and (23.3 $\pm$ 4.8) mGy for Barracuda and Ion Chamber techniques respectively with a mean deviation of 0.67 mGy between them.

Results for the CT body phantom examination showed a minimum $CTDI_{vol}$ deviation of 0.85% between the two techniques when the tube potential and the tube current-time product were set at 130kVp and 80mAs respectively for abdominal examination. When the scan protocol of tube potential and tube current-time product were set at 130kVp and 220mAs respectively for pelvis examination, the maximum $CTDI_{vol}$ deviation was estimated at 8.73%. With a tube potential of 130kVp and tube current-time product of 180mAs for a chest examination, an estimated $CTDI_{vol}$ deviation of -6.47% was recorded between the two techniques. Varying the tube current-time products from 80mAs to

220mAs with a fixed tube potential of 130kVp for body (chest, abdomen, pelvis) phantom examination, the average $CTDI_{vol}$ measured were (21.1 ± 10.6) mGy and (20.7 ± 9.6) mGy for Barracuda and Ion Chamber techniques respectively with an average deviation of 1.4 mGy between them.

For the $CTDI_w$ values of the body phantom, the minimum $CTDI_w$ deviation measured was 3.56% at scan protocol of 130kVp potential and 200mAs tube current-time product for chest examination. The maximum deviation was also -9.53% which was recorded at 130kVp tube potential and tube current-time product of 220mAs for pelvis examination. When the tube potential of 130kVp and current-time product of 120mAs were set for abdomen examination, $CTDI_w$ deviation of 5.87% was estimated. With a fixed tube potential of 130kVp and varying the tube current-time product from 80mAs to 220mAs for the body (chest, abdomen, pelvis) examination, mean $CTDI_w$ measured were (16.6 ± 6.7) mGy and (16.5 ± 7.7) mGy for Barracuda and Ion Chamber techniques respectively with an average deviation of 1.0 mGy between them.

Unlike some theoretically estimated CT dose softwares like the CT – Expo software, the CT dose profiler which is connected with the Barracuda computes CT dose by the actual phantom measurements. Brix et al. in 2004, reported that with theoretically estimated CT dose software, the accuracy of the dose measurement may exceed ± 10 %.

The estimated CTDI values for the CT head and body phantoms from this study can be compared with study by Hasford et al. in 2015. In their CT head and body phantom study, they compared $CTDI_{vol}$ from Ion Chamber technique with that displayed on the CT system console. At scan protocol of 120kVp and 150 mAs, they reported dose measurements of 44.3 mGy from the Ion Chamber technique with a corresponding console displayed value of 42.4 mGy for the head phantom examination at $CTDI_{vol}$ deviation of 4.5%. When scan protocol was set at 120 kVp and 100 mAs for pelvic

examination in their study, the dose measured was 20.08 mGy against a console displayed value of 19.49 mGy which yielded a deviation of 3.1%. The measured doses for the head phantom examination can also be compared with a study by Inkoom et al. in 2014 for adult patients undergoing CT examination in six CT facilities. They reported a diagnostic reference levels ($CTDI_{vol}$) of 39.0 – 58.6 mGy in their study. $CTDI_{vol}$ for tube current-time products from 140 – 200mAs and fixed tube potential of 130 kVp for this study is below the diagnostic reference level reported by Inkoom et al. in 2014 but tube current-time products from 220 – 300 mAs for the head phantom examination with both techniques in this study can satisfactorily be compared with the diagnostic reference levels reported in Inkoom et al. in 2014.

When the measured and Console displayed $CTDI_w$ values were compared for the head phantom examinations at fixed kVp of 130, there were minimum and maximum deviations of 2.24% and 16.01% at 240 mAs and 180 mAs respectively between the Barracuda technique and displayed. The minimum and maximum $CTDI_w$ deviations between the Ion Chamber technique and the displayed were also 1.87% and 14.01% at 280 mAs and 160 mAs respectively. Again, there were minimum and maximum $CTDI_{vol}$ deviations of 0.9% and 9.89% at 240 mAs and 300 mAs respectively between Barracuda and displayed, 1.35% and 4.99% at 180 mAs and 220 mAs respectively between the Ion Chamber technique and displayed.

Also, comparison of measured and displayed $CTDI_w$ for the body phantom examinations at 130kVp, yielded minimum and maximum deviations of 0.22% and 9.95% at 100 mAs and 200 mAs respectively between Barracuda and displayed and -0.67 and 15.85% at 210 mAs and 120 mAs respectively between the Ion Chamber technique and displayed. The minimum and maximum $CTDI_{vol}$ deviations were also -2.33% and 12.15% at 220 mAs and 180 mAs respectively between Barracuda technique and displayed, -1.28% and 9.82% at 160 mAs and 100 mAs respectively between Ion Chamber technique and displayed. Descamps et al. in 2012, estimated percentage deviations between

measured and console displayed doses for new generation CT scanners. Findings from their study shows that measured doses ($CTDI_{vol}$) for CT examinations could be as much as 32 – 35% higher or lower than console displayed doses.

Comparison of results from this research work to some international diagnostic reference levels (DRLs) for Europe (Bongartz et al., 2004), United Kingdom (Shrimpton, 2004) and American College of Radiology (ACR, 2008) is presented in Table 2.23.

Table 4.25: Comparison of $CTDI_{vol}$ from this study with some international diagnostic reference levels

	$CTDI_{vol}$ (mGy)				
Examination	**This study (Barracuda)**	**This study (Ion Chamber)**	**Europe - 2004 (Bongartz et al., 2004)**	**UK - 2003 (Shrimpton, 2004)**	**ACR - 2008 [ACR (2008)]**
Head	32.90 – 53.0	32.24 – 56.42	60	65 – 100	75
Abdomen	9.5 – 15.6	9.42 – 15.24	25	14	25

The smallest dose of 32.9mGy from the Barracuda technique was observed to be 82%, 98 – 204% and 127 % lesser in comparison to the diagnostic reference levels for Europe (2004), UK (2003) and ACR (2008) respectively whilst the highest dose of 53mGy was also observed to be 13%, 23 – 89% and 42% lesser in comparison to the diagnostic reference levels for Europe (2004), UK (2003) and ACR (2008) for the head phantom examination. The smallest dose, 32.24mGy estimated from the Ion Chamber technique was 86%, 102 – 210% and 132% lesser in comparison to the above stated international diagnostic reference levels for Europe (2004), UK (2003) and ACR (2008) respectively for the head phantom examination. The highest dose estimated from the Ion Chamber technique for

the head phantom examination was also 6%, 15 – 77%, 33% lesser in comparison to the stated international diagnostic reference levels for Europe (2004), UK (2003) and ACR (2008) respectively.

For the abdomen examination, the smallest dose of 9.5mGy recorded from the Barracuda technique was 163%, 47% and 163% lesser in comparison with DRLs for Europe (2004), UK (2003) and ACR (2008) diagnostic reference levels. The highest dose, 15.6 mGy recorded with the Barracuda for the abdomen examination was also 60% lesser than DRLs for both Europe (2004) and ACR (2008) and 10% higher than DRL for UK (2003). Also, the smallest dose of 9.42 mGy estimated with the Ion Chamber technique from the abdomen examination was 165%, 49% and 165% when compared with DRLs for Europe (2004), UK (2003) and ACR (2008) respectively. The highest dose of 15.24 mGy was also 64% lesser for both DRLs for Europe (2004) and ACR (2008) and 8% higher than DRL for UK (2003). Comparison of $CTDI_w$ values from this study with some international diagnostic reference levels can also be seen in Table 4.24.

Table 4.26: Comparison of $CTDI_w$ from this study with some international diagnostic reference levels

	$CTDI_w$ (mGy)				
Examination	**This study (Barracuda)**	**This study (Ion Chamber)**	**Germany- 2003 (Brix, 2003)**	**Taiwan - 2007 (Tsai et al., 2007)**	**Switzerland - 2004 (Aroua et al., 2004)**
Head	17.6 – 29.12	17.73 – 31.03	60	75	60
Abdomen	8.0 – 13.0	7.54 – 12.19	25	31	20

The smallest $CTDI_w$ of 17.6 mGy from the Barracuda technique was observed to be 241%, 326% and 241 % lesser in comparison to the diagnostic reference levels for Germany (2003), Taiwan (2007) and

Switzerland (2004) respectively whilst the highest dose of 29.12 mGy was also observed to be 106%, 158% and 106% lesser in comparison to the diagnostic reference levels for Germany (2003), Taiwan (2007) and Switzerland (2004) for the head phantom examination. The smallest dose, 17.73 mGy estimated from the Ion Chamber technique was 238%, 323% and 238% lesser in comparison to the above stated international diagnostic reference levels for Germany (2003), Taiwan (2007) and Switzerland (2004) respectively for the head phantom examination. The highest dose, 31.03 mGy estimated from the Ion Chamber technique for the head phantom examination was also 93%, 142%, 93% lesser in comparison to the stated international diagnostic reference levels for Germany (2003), Taiwan (2007) and Switzerland (2004) respectively.

For the body (abdomen) examination, the smallest dose of 8.0 mGy recorded from the Barracuda technique was 213%, 288% and 150% lesser in comparison with DRLs for Germany (2003), Taiwan (2007) and Switzerland (2004) diagnostic reference levels. The highest dose, 13 mGy recorded with the Barracuda for the abdomen examination was also 92%, 138% and 54% lesser in comparison with DRLs for both Germany (2003), Taiwan (2007) and Switzerland (2004). Also, the smallest $CTDI_w$ of 7.54 mGy estimated with the Ion Chamber technique from the abdomen examination was 232%, 311% and 165% lesser when compared with DRLs for Germany (2003), Taiwan (2007) and Switzerland (2004) respectively. The highest dose of 12.19 mGy was also 105%, 154% and 64% lesser in comparison with DRLs for Germany (2003), Taiwan (2007) and Switzerland (2004) respectively. Even though, there are varying differences between the doses measured with the Barracuda and Ion Chamber with the DRLs for Europe (2004), UK (2003) and ACR (2008), they do not imply overdosing or underdosing the international protocols to patients since the phantoms used in this study were simple homogeneous PMMA.

4.4 Limitations with CTDI Measurement Techniques

CTDI provides CT users with a good estimate of the CT scanner output. However, there are associated limitations.

- CTDI is usually measured using cylindrical, homogenous PMMA phantoms which arguably represents the dose to objects of different attenuation or size like that of the human body.
- Moreover, the charges recorded by the Ion Chamber during the CTDI measurement are converted to exposure which is subsequently converted to dose to air by a conversion factor. Hence, the CTDI measured from the technique is expressed as dose to air and not dose to tissue, thus, limiting its importance in tissue dosimetry even though, Monte Carlo simulation is mostly used to estimate organ doses for different volumes of the human system.
- The CTDI represents the dose to the whole scan volume and does not indicate the dose to a particular point of interest in the scan volume should the patient table remain stationary for scans such as that required in perfusion CT.

CHAPTER FIVE

5 CONCLUSION AND RECOMMENDATIONS

5.1 Overview

This chapter recaps the study by presenting the conclusion and recommendations. This chapter assesses the objectives to see whether they were met and recommendations for further study were also presented here.

5.2 Conclusion

The results of the study show that $CTDI_w$ and $CTDI_{vol}$ have been successfully estimated using both devices and techniques described in the research methodology as stated in the study objectives. The $CTDI_w$ and $CTDI_{vol}$ estimations by the Ion Chamber technique were done by setting parameters such as the tube potential (130kVp), slice thickness (4mm and 5mm) and pitch factor (0.55 and 0.8) constant whiles varying the current-time products from 80 – 300mAs to record charges for both head and body phantoms. Formalism from AAPM Report 96 (AAPM, 2008) to convert charges recorded to exposure and subsequently to CTDI.

The $CTDI_w$ and $CTDI_{vol}$ estimations by the dose profiler probe were automatically generated by the Barracuda when the scan protocols that were used with the Ion Chamber technique were entered. The minimum and maximum deviations recorded from both techniques were estimated to be 0.69% and -6.56% respectively for $CTDI_w$ and 0.61% and -6.45% for $CTDI_{vol}$ for head phantom examination. These results were comparable to work done by other researches and was within acceptable ranges from existing CT literature.

Measurements for head phantom examination showed a minimum and maximum deviations of 3.56% and -9.53% respectively for $CTDI_w$ and 0.85% and 8.73 for $CTDI_{vol}$ for the head phantom examination. These results were also favorably comparable to values from other retrospective studies.

In comparison to the average and 75th percentile values of some international diagnostic reference levels (DRLs) which used exposure parameter of 130kVp and current-time products between 230 – 250mAs, the highest $CTDI_{vol}$ obtained were 13 – 89% and 6 – 77% lesser for Barracuda and Ion Chamber techniques respectively for head phantom examination. With the body phantom examination (abdomen scan technique), the highest dose from the Barracuda technique was 64% lesser and 8% higher in comparison to some international diagnostic reference levels. The differences between the estimated CTDI values from this study and that from the international levels do not imply overdosing and underdosing of patients in those countries where the reference levels were recorded. The differences were said to have occurred due to the standardization and homogeneous nature of the phantoms used as compared to the different size of tissue and their respective attenuations in the human system.

The results therefore showed that the PTW Ion Chamber validated the CTDI values obtained from the Barracuda technique. The Ion Chamber technique confirms the degree of confidence in the Barracuda for CT dose measurements. For routine clinical environment, any of the two devices or methods can be used adequately to give the needed dose information from the CT scanners.

The concept of accuracy was not applicable in this study, since, there is a range of dose values acceptable from a CT scanner to yield quality of image with optimum diagnostic information.

5.3 Recommendation

The following recommendations are made to individual parties involved in the use, optimizing of radiation dose and protection of patients.

5.3.1 Sweden Ghana Medical Centre

This study was conducted at a fixed tube potential for all the devices and techniques involved. It is recommended the medical physicists at Sweden Ghana Medical Center (SGMC) investigate further with adjusted or varying tube potentials in order to see the effect of different potentials on the CTDI values obtained from the two techniques.

5.3.2 Radiological and Medical Sciences Research Institute (RAMSRI)

In order to be sure of optimum radiation output from a CT scanner, there is always the need to measure its radiation dose. It is recommended the RAMSRI use the acquired PTW CT pencil Ion Chamber to validate the dose measured with other techniques at different CT imaging centers to help enhance the degree of confidence in the existing techniques. This would also help to assess the efficiency of the PTW ion chamber under different conditions of Pressure and Temperature in other CT rooms

5.3.3 Research Community

It is recommended further study be done in comparing CTDI values from both the Ion Chamber and Barracuda with that displayed on the CT consoles for different tube potentials and tube current-time products. It will be expedient to know the amount of deviations the CT console displayed values will be from both the Ion Chamber and Barracuda techniques at varying kVp.

REFERENCES

AAPM (1990). "Computers in Medical Physics," in *AAPM summer school proceedings,* Benedetto, A.R., Huang, H.K. and Ragan, D.P., eds. (American Institute of Physics, New York).

AAPM (1993) "The Physics of MRI," in *AAPM summer school proceedings*, Bronskill, M.J. and Sprawls, P., Eds. (American Institute of Physics, New York).

AAPM. (2008). The Measurement, Reporting, and Management of Radiation Dose in CT (AAPM Report No.69). *Report of AAPM Task Group 23 of the Diagnostic Imaging Council CT Committee*.

AAPM. (2008). The Measurement, Reporting, and Management of Radiation Dose in CT (AAPM Report No.96). *Report of AAPM Task Group 23 of the Diagnostic Imaging Council CT Committee*.

AAPM. (2011). Site specific dose estimates (SSDE) in paediatric and adult body CT examinations (AAPM Report No. 204). *Report of AAPM Task Group 204 of AAPM. College Park, MD.*

American College of Radiology, "ACR Practice Guideline for Diagnostic Reference Levels in Medical X-Ray Imaging," 2002 (revised 2008)

Aroua, A., Besancon, A., Buchillier-Decka I., et al. (2004). Adult reference levels in diagnostic and interventional radiology for temporary use in Switzerland, *Radiation Protection Dosimetry,* 111(3): 289 - 295.

Aweda, M. A., & Arogundade, R. (2007). Patient dose reduction methods in computerized tomography procedures: A review. *Academic Journals*, *2*(1), 1– 9. Retrieved March 3, 2016 from http://www.academicjournals.org/article/article1380202111_Aweda and Arogundade.pdf

Bauhs, J. A., Vrieze, T. J., Primak, A. N., Bruesewitz, M. R., & McCollough, C. H. (2008). CT dosimetry: comparison of measurement techniques and devices. *Radiographics*, 28 (1): 245 - 253

Bongartz, G., Golding, S. J., Jurik, A. G., M. Leonardi, Meerten, E. V. P. V., Rodríguez, R., Tosi, G. (2004). Introduction to multi slice computed tomography (MSCT). *European Guidelines for Multi-slice Computed Tomography*

Brenner, D. J., & Hall, E. J. (2007). Computed tomography--an increasing source of radiation exposure. *The New England Journal of Medicine*, *357*(22): 2277–2284. http://doi.org/10.1056/NEJMra072149

Brix, G., Nissen-Meyer, S., Lechel, U., Nissen-Meyer, J., Griebel, J., Nekolla, E. A, … Reiser, M. (2009). Radiation exposures of cancer patients from medical X-rays: how relevant are they for individual patients and population exposure? *European Journal of Radiology*, *72*(2): 342–7. http://doi.org/10.1016/j.ejrad.2008.07.009

Brix, G. (2003). Notice of diagnostic reference values for radiology and nuclear medicine studies. *Federal Office for Radiation Protection*, ed. Germany; 2003.

Bushberg, J. T., Seibert, J. A., Leidholdt, E. M., & Boone, J. M. (2011a). *The essential physics of medical imaging*. *Lippincott Williams & Wilkins* (1st ed.). Hall, New York. Retrieved March 2, 2016 from http://www.lww.com/Product/9780781780575 VN - readcube.com

Bushberg, J. T., Seibert, J. A., Leidholdt, E. M., & Boone, J. M. (2011b). *The essential physics of medical imaging*. *Lippincott Williams & Wilkins* (second edi). Retrieved March 2, 2016 from http://www.lww.com/Product/9780781780575 VN - readcube.com

Carlton, R. R., Adler, A. M., & Bushong, S. (2005). *Principles of radiographic imaging.*

Catalano, C., Francone, M., Ascarelli, A., Mangia, M., Iacucci, I., & Passariello, R. (2007). Optimizing radiation dose and image quality. *European Radiology, Supplement*, *17*(SUPPL. 6), 26–32. http://doi.org/10.1007/s10406-007-0225-6

Cunningham, I. A., & Judy, P. F. (2000). *Computed Tomography J. D. Bronzino (Ed.)The Biomedical Engineering Handbook*. (J. D. Bronzino, Ed.) (Second Edi). Retrieved from Retrieved from http://sm-7.net/upload/Detali mashin/bmt/The Biomedical Engineering Handbook - 2Ed - Bronzino/ch062.pdf

Descamps, C., Gonzalez, M., Garrigo, E., Germanier, A., & Venencia, D. (2012). Measurements of the dose delivered during CT exams using AAPM task group report No. 111. *Journal of Applied Clinical Medical Physics*, 13 (6): 3934 - 3942.

Dixon, R.L., (2006) "Restructuring CT dosimetry – A realistic strategy for the future requiem for the pencil chamber," *Medical Physics*. 33(10), 3973-3976.

Fishman, E. K., & Jeffrey, R. B. (1998). *Spiral CT: principles, techniques, and clinical applications:* Lippincott-Raven Philadelphia.

Fujii, K., Aoyama, T., Yamauchi-Kawaura, C., Koyama, S., Yamauchi, M., Ko, S., … Nishizawa, K. (2009). Radiation dose evaluation in 64-slice CT examinations with adult and paediatric anthropomorphic phantoms. *British Journal of Radiology*, *82*(984), 1010–1018

GE, H. C. (2003). CT: Radiation Safety and Applications. Retrieved March 3, 2016 from http://www.gehealthcare.com/gecommunity/tip_tv/subscribers/sup_material/supplement/2249.pdf

Goergen, S., Revell, A., & Walker, C. (2009). Computed Tomography (CT). *Inside Radiology*. Retrieved March 2, 2016 from http://www.nibib.nih.gov/science-education/science topics/computed tomography-ct

Goldman, L. W. (2008). Principles of CT: multi-slice CT. *Journal of Nuclear Medicine Technology, 36*(2), 57.

Hall, E. J., & Brenner, D. J. (2008). Cancer risks from diagnostic radiology. *British Journal of Radiology*, *81*(965), pp 362–378. http://doi.org/10.1259/bjr/01948454

Hanafi, A. M. (2005). *Trends in CT abdominal doses in Malaysian practices*. *Doctor of Health Science*. University of Sydney. Retrieved from http://www.biomedsearch.com/sci/Trends-in CT-abdominaldoses/0003507437.html

Hasford, F., Wyk, B. V., Mabhengu T., Vangu, M. D. T., Kyere, A. K., Amuasi, J. H. (2015). Determination of dose accuracy in CT examinations. *Journal of Radiation Research and Applied Sciences*, 8(4): 489 – 492.

IEC (2002) "Medical electrical equipment, Part 2-44: Particular requirements for the safety of X-ray equipment for computed tomography," in *Publication No. 60601 2nd ed.*, (International Electrotechnical Commission, Geneva, Switzerland).

IEC (2003) "Amendment 1: Medical electrical equipment, Part 2-44: Particular requirements for the safety of X-ray equipment for computed tomography." in *IEC publication No.60601-amd1, ed. 2.1* (International Electrotechnical Commission, Geneva, Switzerland).

Jessen, K. A., Panzer, W., Shrimpton, P. C., Bongartzm, G., Geleigns, J., Golding, S. J., Jurik, A. G., Leonar, M. & Tosi, G. (2000). In *Office for Official Publications of the European Communities*, Luxembourg.

Jurik, A. G., Jessen, K. A, & Hansen, J. (1997). Image quality and dose in computed tomography. *European Radiology*, *7*(1): 77–81. http://doi.org/10.1007/s003300050114

Kalender, W. A. (2005). CT: the unexpected evolution of an imaging modality. *European Radiology*, *15*(Suppl 4), D21–4. http://doi.org/10.1007/s10406-005-0128-3

Kalra, M. K., Maher, M. M., Toth, T. L., Hamberg, L. M., Blake, M. A., Shepard, J.-A., & Saini, S. (2004). Strategies for CT radiation dose optimization. *Radiology*, *230*(3): 619–628. http://doi.org/10.1148/radiol.2303021726

Katada, K. (2002). Characteristics of multislice CT. *Acute Myocardial Infarction*, 175.

Kulama, E. (2004). Scanning protocols for multislice CT scanners. *British Journal of Radiology*, *77*(SPEC. ISS.). http://doi.org/10.1259/bjr/28755689

Lechel, U., Becker, C., Langenfeld-Jäger, G., & Brix, G. (2009). Dose reduction by automatic exposure control in multidetector computed tomography: comparison between measurement and calculation. *European Radiology*, *19*(4): 1027–34. http://doi.org/10.1007/s00330 008-1204-6

Leitz, W., Axelsson, B. & Szendrö, G. (1995) "Computed tomography dose assessment: a practical approach," *Radiation Protection and Dosimetry,* 57(1-4): 377-380.

Lewis, M. A. & Edyvean, S. (2005). Patient dose reduction in CT. *The British Journal of Radiology*, *78*(934): 880–883. http://doi.org/10.1259/bjr/75960844

Mahesh, M. (2009). *MDCT Physics: The Basics--Technology, Image Quality and Radiation Dose*: Lippincott Williams & Wilkins

Marchal, T. J. Vogl, J. P. & Heiken, G. D. R. (2005). *Multidetector-Row Computed Tomography: Scanning and Contrast Protocols Barnes & Noble*. *Springer*. Springer Verlag. http://doi.org/9788847003057

McCollough, C.H. and Zink, F.E., (1999) "Performance evaluation of a multi-slice CT system," *Med. Phys.* 26(11): 2223-2230. doi:10.1118/1.598777

McCollough, C. H., Primak, A. N., Braun, N., Kofler, J., Yu, L., & Christner, J. (2009). Strategies for reducing radiation dose in CT. *Radiologic Clinics of North America*, *47*(1): 27–40. http://doi.org/10.1016/j.rcl.2008.10.006

McNitt-Gray M.F., (2002) "AAPM/RSNA Physics Tutorial for Residents: Topics in CT. Radiation dose in CT," *Radiographics* 22(6): 1541-1553. doi:10.1148/rg.226025128

Mettler, F., Weist, P., & Locken, J. (2000). CT Scanning:Patterns of use and dose. *Journal of Radiological Protection*, *20*(4): 353–359.

Mulkens, T., Salgado, R., & Bellinck, P. (2007). Dose optimization and reduction in CT of the head and neck, including brain. Radiation Dose from Adult and Pediatric Multidetector Computed Tomography, 135–151.

Nagel, H.D., (2000) *Radiation exposure in computed tomography,* (European Coordination Committee of the Radiological, Electromedical and Healthcare IT Industry (COCIR), Frankfurt, Germany).

Nations, U., Nations, U., Committee, S., & Radiation, A. (2010). Sources and effects of ionizing radiation *United Nations Scientific Committee on the Effects of Atomic Radiation*. *Medical radiation exposureNew York, NY: United Nations* (Vol. I). Retrieved from http://www.unscear.org/unscear/en/publications.html

Rehani, M. M., & Berry, M. (2000). Radiation doses in computed tomography. *BMJ, 320*(7235): 593.

Seeram, E. (2009). *Computed tomography: physical principles, clinical applications, and quality control* ((third ed)). USA.

Siemens. (2010). Computed Tomography; Its History and Technology. *Siemens Medical*, 1–36. Retrieved March 1, 2016 from www.SiemensMedical.com

Shrimpton, P. C. (2004). Assessment of Patient Dose in CT. *National Radiological Protection Board*, 5(5): 1–36.

Shrimpton P., "Assessment of Patient Dose in CT" in Bongart G.Z., Golding S.J., Jurik A.G., et al. (2004). *European Guidelines for Multislice Computed Tomography*, 2004.

Shope, T. B., Gagne, R. M., & Johnson, G. C. (1981). A method for describing the doses delivered by transmission x-ray computed tomography. *Medical Physics*, 8(4): 488 - 495.

Tsai, H. Y., Tung, C. J., Yu, C. C. & Tyan, Y. S. (2007). Survey of computed tomography scanners in Taiwan: dose descriptors, dose guidance levels, and effective doses," *Medical Physics,* 34(4): 1234 - 1243.

Tsapaki, V. & Rehani, M. (2007). Dose management in CT facility. *Biomedical Imaging and Intervention Journal*, *3*(2), e43. http://doi.org/10.2349/biij.3.2.e43

United States FDA (1984) *Code of Federal Regulations*, *CFR* 21(2): 1020-1033.

UNSCEAR. (2000). *Report to the general assembly, Annex D: medical radiation exposures*. N.Y: United Nations 2000.

APPENDICES

Appendix A:

Typical Effective Dose Values for Some CT and Non-CT Imaging Examinations	
Imaging Examinations	Typical Effective Dose Values (mSv)
Non-CT Studies	
Hand radiography	< 0.1
Dental Bitewing radiography	< 0.1
Chest radiography	0.1 – 0.2
Mammography	0.3 – 0.6
Lumbar spine radiography	0.5 – 1.5
Barium enema radiography	3 – 6
Coronary angiography (diagnostic)	5 – 10
Sestamibi myocardial perfusion study	13 – 16
Thallium myocardial perfusion study	35 – 40
CT Studies	
Head CT	1 – 2
Chest CT	5 – 7
Abdominal CT	5 – 7
Pelvic CT	3 – 4
Abdominal and Pelvic CT	8 – 12
Coronary artery calcium CT study	1 – 3
Coronary CT angiography	5 – 14

Appendix B:

Charges recorded for CT head phantom examination from PTW electrometer											
Fixed kVp	**Varying mAs**	**Recorded Charges**									
		Central (C) [nC]		Periphery (1) [nC]		Periphery (2) [nC]		Periphery (3) [nC]		Periphery (4) [nC]	
		1	2	1	2	1	2	1	2	1	2
130	140	0.1314	0.1314	0.1613	0.1617	0.1626	0.1630	0.1638	0.1638	0.1634	0.1634
130	160	0.1320	0.1320	0.1620	0.1624	0.1633	0.1637	0.1646	0.1646	0.1641	0.1641
130	180	0.1478	0.1478	0.1814	0.1819	0.1829	0.1834	0.1843	0.1843	0.1838	0.1838
130	200	0.1541	0.1541	0.192	0.1950	0.1941	0.1950	0.1956	0.1956	0.1952	0.1952
130	220	0.1643	0.1643	0.2016	0.2021	0.2032	0.2037	0.2048	0.2048	0.2043	0.2043
130	240	0.1807	0.1807	0.2218	0.2223	0.2235	0.2241	0.2253	0.2253	0.2247	0.2247
130	260	0.1971	0.1971	0.2419	0.2426	0.2438	0.2445	0.2458	0.2458	0.2451	0.2451
130	280	0.2135	0.2135	0.2621	0.2628	0.2642	0.2649	0.2662	0.2662	0.2655	0.2655
130	300	0.2300	0.2300	0.2822	0.2830	0.2845	0.2852	0.2867	0.2867	0.2860	0.2860

Appendix C:

Charges recorded for CT body phantom examination from PTW electrometer												
Fixed kVp	**Varying mAs**	**Examination**	**Recorded Charges**									
			Central (C) [nC]		Periphery (1) [nC]		Periphery (2) [nC]		Periphery (3) [nC]		Periphery (4) [nC]	
			1	2	1	2	1	2	1	2	1	2
130	80	A	0.0665	0.0670	0.0885	0.0880	0.0885	0.0885	0.0875	0.0875	0.0880	0.0880
130	100	A	0.0899	0.0899	0.0940	0.0938	0.0942	0.0942	0.0944	0.0946	0.0938	0.0938
130	120	A	0.1079	0.1079	0.1128	0.1126	0.1130	0.1130	0.1133	0.1135	0.1126	0.1126
130	140	A	0.1271	0.1271	0.1328	0.1327	0.1330	0.1328	0.1329	0.1329	0.1331	0.1330
130	160	C	0.1500	0.1500	0.1860	0.1862	0.1862	0.1859	0.1859	0.1865	0.1860	0.1861
130	180	C	0.1688	0.1688	0.2093	0.2095	0.2095	0.2091	0.2091	0.2098	0.2093	0.2094
130	200	C	0.1875	0.1875	0.2325	0.2328	0.2328	0.2324	0.2324	0.2331	0.2325	0.2326
130	210	P	0.2410	0.2410	0.3150	0.3152	0.3150	0.3152	0.3148	0.3148	0.3154	0.3152
130	220	P	0.2560	0.2560	0.3300	0.3300	0.3310	0.3311	0.3310	0.3312	0.3315	0.3315